

# $\varepsilon'/\varepsilon$ and Rare K and B Decays in the MSSM

A.J. Buras<sup>1</sup>, P. Gambino<sup>2</sup>, M. Gorbahn<sup>1</sup>,  
S. Jäger<sup>1</sup> and L. Silvestrini<sup>1,3</sup>

<sup>1</sup> Physik Department, Technische Universität München,  
D-85748 Garching, Germany

<sup>2</sup> Theory Division, CERN, CH-1211 Geneva 23, Switzerland

<sup>3</sup> Dipartimento di Fisica, Università di Roma “La Sapienza” and  
INFN, Sezione di Roma, P.le A. Moro, I-00185, Roma, Italy

## Abstract

We analyze the CP violating ratio  $\varepsilon'/\varepsilon$  and rare K and B decays in the MSSM with minimal flavour and CP violation, including NLO QCD corrections and imposing constraints on the supersymmetric parameters coming from  $\varepsilon$ ,  $B_{d,s}^0 - \bar{B}_{d,s}^0$  mixings,  $B \rightarrow X_s \gamma$ ,  $\Delta \rho$  in the electroweak precision studies and from the lower bound on the neutral Higgs mass. We provide a compendium of phenomenologically relevant formulae in the MSSM. Denoting by  $T(Q)$  the MSSM prediction for a given quantity normalized to the Standard Model result we find the ranges:  $0.53 \leq T(\varepsilon'/\varepsilon) \leq 1.07$ ,  $0.65 \leq T(K^+ \rightarrow \pi^+ \nu \bar{\nu}) \leq 1.02$ ,  $0.41 \leq T(K_L \rightarrow \pi^0 \nu \bar{\nu}) \leq 1.03$ ,  $0.48 \leq T(K_L \rightarrow \pi^0 e^+ e^-) \leq 1.10$ ,  $0.73 \leq T(B \rightarrow X_s \nu \bar{\nu}) \leq 1.34$  and  $0.68 \leq T(B_s \rightarrow \mu \bar{\mu}) \leq 1.53$ . We point out that these ranges will be considerably reduced when the lower bounds on the neutral Higgs mass and  $\tan \beta$  improve. Some contour plots illustrate the dependences of the quantities above on the relevant supersymmetric parameters. As a byproduct of this work we update our previous analysis of  $\varepsilon'/\varepsilon$  in the SM and find in NDR  $\varepsilon'/\varepsilon = (9.2^{+6.8}_{-4.0})$ , a value 15% higher than in our 1999 analysis.

# 1 Introduction

One of the present central issues of particle physics phenomenology is the question whether the size of the experimentally observed direct CP violation in  $K_L \rightarrow \pi\pi$  decays can be described within the Standard Model (SM).

The most recent experimental results for the ratio  $\varepsilon'/\varepsilon$ , which measures the size of the direct CP violation in  $K_L \rightarrow \pi\pi$  relative to the indirect one, read:

$$\text{Re}(\varepsilon'/\varepsilon) = \begin{cases} (28.0 \pm 4.1) \cdot 10^{-4} & \text{(KTeV) [1]} \\ (14.0 \pm 4.3) \cdot 10^{-4} & \text{(NA48) [2]}. \end{cases} \quad (1.1)$$

Together with the older NA31 measurement  $((23 \pm 7) \cdot 10^{-4})$  [3], these data confidently establish direct CP violation in nature and taking also the E731 result  $((7.4 \pm 5.9) \cdot 10^{-4})$  [4] into account one finds the grand average

$$\text{Re}(\varepsilon'/\varepsilon) = (19.2 \pm 2.4) \cdot 10^{-4} \quad \text{with} \quad \chi^2/ndf = 11.1/5 \quad (1.2)$$

close to the NA31 result.

There are different opinions whether the grand average in (1.2) can be accommodated within the SM. We list the results from various groups in table 1. The labels (MC) and (S) in the second column stand for two error estimates: “Monte Carlo” and “Scanning” respectively. The result from the Munich group given here is an update of the analysis in [5] done in the present paper. Similarly the result of the Rome group is the most recent estimate given in [6]. We do not list the values of the non-perturbative parameters  $B_6^{(1/2)}$  and  $B_8^{(3/2)}$  used in different analyses as the comparison of these values could be misleading. The reason is that in certain papers these factors are  $m_s$ -independent and in other papers they depend on  $m_s$ . Typically  $B_6^{(1/2)} = 0.8 - 1.6$  and  $B_8^{(3/2)} = 0.6 - 1.2$ . Exceptions are the analyses in [7] and [8] where  $B_6^{(1/2)}$  in the ballpark of 3 can be found.

In [5, 6, 9]  $\varepsilon'/\varepsilon$  has been found to be typically a factor of 2 below the data and the KTeV result in (1.1) could only be accommodated if all relevant parameters were chosen simultaneously close to their extreme values. On the other hand the NA48 result is essentially compatible with [5, 6, 9] within experimental and theoretical errors. Higher values of  $\varepsilon'/\varepsilon$  than in [5, 6, 9], in the ballpark of (1.2), have been found in [7, 8, 10-13]. The result in [14] corresponds to  $B_6^{(1/2)} = B_8^{(3/2)} = 1$  (see section 7.1) as the Dubna-DESY group has no estimate of these non-perturbative parameters. Recent reviews can be found in [6, 10, 15]. Furthermore it has also been suggested that final state interactions (FSI) could enhance  $\varepsilon'/\varepsilon$  by a factor of two [10, 13, 16]. A critical analysis of this suggestion has been presented in [17]. In our opinion the issue of the size of FSI in the evaluation of  $\varepsilon'/\varepsilon$  is still an open question. An interesting recent proposal in [18], if realized, could put

Reference	$\varepsilon'/\varepsilon$ [ $10^{-4}$ ]
Munich [5]	$9.2^{+6.8}_{-4.0}$ (MC)
Munich [5]	$1.4 \rightarrow 32.7$ (S)
Rome [6, 9]	$8.1^{+10.3}_{-9.5}$ (MC)
Rome [6, 9]	$-13.0 \rightarrow 37.0$ (S)
Trieste [10]	$22 \pm 8$ (MC)
Trieste [10]	$9 \rightarrow 48$ (S)
Dortmund [11]	$6.8 \rightarrow 63.9$ (S)
Montpellier [7]	$24.2 \pm 8.0$
Granada-Lund [8]	$34 \pm 18$
Dubna-DESY [14]	$-3.2 \rightarrow 3.3$ (S)
Taipei [12]	$7 \rightarrow 16$
Barcelona-Valencia [13]	$17 \pm 6$

Table 1: Results for  $\varepsilon'/\varepsilon$  in the SM in units of  $10^{-4}$ .

the inclusion of FSI in the lattice calculations of hadronic matrix elements in principle under control.

While all theoretical analyses quoted above use the NLO short distance Wilson coefficients of [19-23], they differ in the evaluation of the hadronic matrix elements of the relevant operators. Being of non-perturbative origin, the latter calculations suffer from large theoretical uncertainties, which at present preclude any firm prediction of  $\varepsilon'/\varepsilon$  within the SM and its extensions. In this context, the matching between the short distance calculations of Wilson coefficients and the long distance estimates of hadronic matrix elements is not fully under control. In particular, it is crucial that these two calculations are performed in the same renormalization scheme [24]. Moreover it has been pointed out recently in [25] that the presence of higher dimensional operators can in the case of low matching scales complicate further this issue. Finally, there is the question of isospin breaking effects that could be more important than initially thought but are difficult to estimate [26, 27]. There is a hope, however, that in the coming years the situation may improve through advanced lattice simulations and new analytical studies.

In any case in view of the very large theoretical uncertainties and sizable experimental errors there is still a lot of room for non-standard contributions to  $\varepsilon'/\varepsilon$ . Indeed the results from NA31, KTeV and NA48 prompted several analyses of  $\varepsilon'/\varepsilon$  within various extensions of the SM like general supersymmetric models [28-32], models with anomalous gauge couplings [33], four-generation models [34] and models with additional fermions and gauge

bosons [35]. Unfortunately several of these extensions have many free parameters and these studies are not very conclusive at present. The situation may change in the future when new data from high energy colliders will restrict the possible ranges of parameters involved. For instance a very recent analysis of the bounds on anomalous gauge couplings from LEP2 data indicates that substantial enhancements of  $\varepsilon'/\varepsilon$  from this sector are very unlikely [36].

On the other hand it appears that the  $\varepsilon'/\varepsilon$  data puts models in which there are new positive contributions to  $\varepsilon$  and negative contributions to  $\varepsilon'$  in difficulties. In particular as analyzed in [5] the two Higgs Doublet Model II can either be ruled out with improved hadronic matrix elements or a powerful lower bound on  $\tan\beta$  can be obtained from  $\varepsilon'/\varepsilon$ . In the Minimal Supersymmetric Standard Model (MSSM), in addition to charged Higgs exchanges in loop diagrams, also charginos contribute. For a suitable choice of the supersymmetric parameters, the chargino contribution can enhance  $\varepsilon'/\varepsilon$  with respect to the SM expectations [37]. Yet, as found in [37], the most conspicuous effect of minimal supersymmetry is a depletion of  $\varepsilon'/\varepsilon$ . The situation can be different in more general models in which there are more parameters than in the two Higgs doublet model II and in the MSSM, in particular new CP violating phases. As an example, in general supersymmetric models  $\varepsilon'/\varepsilon$  can be considerably enhanced through the contributions of the chromomagnetic penguins [28-30, 38],  $Z^0$ -penguins with the opposite sign to the one in the SM [30, 39-41] and isospin breaking effects [31].

The purpose of the present paper is a new analysis within the MSSM with minimal flavour violation, which updates and generalizes the work of Gabrielli and Giudice [37]. Compared to the latter paper, the main new ingredients of our analysis are:

- The inclusion of NLO-QCD and QED corrections;
- the update in the CKM and non-perturbative parameters;
- the imposition of constraints on supersymmetric parameters coming in particular from  $\Delta\rho$  in the electroweak precision studies and from the lower bound on the neutral Higgs mass, in addition to the ones provided by the  $B \rightarrow X_s \gamma$  decay rate;
- the simultaneous study of the rare decays  $K^+ \rightarrow \pi^+ \nu \bar{\nu}$ ,  $K_L \rightarrow \pi^0 \nu \bar{\nu}$ ,  $K_L \rightarrow \pi^0 e^+ e^-$ ,  $B \rightarrow X_s \nu \bar{\nu}$  and  $B_s \rightarrow \mu \bar{\mu}$  which are sensitive to  $Z^0$ -penguin contributions.

As in [37] we will consider the MSSM with minimal flavour violation, in which the effective local operators are the same as in the SM and the only source of CP violation is the KM phase. Since the supersymmetric particles have masses  $\mathcal{O}(M_W)$  or higher and the effective low energy operators are the same as in the SM, the impact of new contributions

in a renormalization group analysis is only felt in the initial conditions for the Wilson coefficients taken usually at  $\mu = \mathcal{O}(M_W)$ . The renormalization group transformation from  $\mu = \mathcal{O}(M_W)$  down to  $\mu = \mathcal{O}(1 \text{ GeV})$  is on the other hand the same as in the SM. This simplifies the inclusion of QCD corrections considerably.

In view of the fact that the new contributions enter only the initial conditions for the Wilson coefficients it is useful to follow [42] and to cast the expression for  $\varepsilon'/\varepsilon$  into a formula which exhibits transparently the new supersymmetric contributions. One finds [5]

$$\varepsilon'/\varepsilon = \text{Im}\lambda_t \cdot F_{\varepsilon'} , \quad F_{\varepsilon'} = P_0 + \sum_r P_r F_r \quad (1.3)$$

where  $\lambda_t = V_{td}V_{ts}^*$ . The coefficients  $P_i$  depend on non-perturbative parameters and include NLO-QCD and QED corrections. They are common to the SM and the MSSM. The functions  $F_r$  resulting from various box and penguin diagrams contain both the SM and supersymmetric contributions involving new exchanges such as charged Higgs particles, charginos, squarks etc. They depend, in addition to  $m_t$ , on the masses of the new particles as well as on a number of other supersymmetric parameters. The explicit expressions for  $F_r$  and the numerical values for the coefficients  $P_i$  will be given in sections 3 and 4 respectively.

There are many new contributions in the MSSM such as charged Higgs, chargino, neutralino and gluino contributions. However, in the case of minimal flavour and CP violation it is a good approximation to keep only charged Higgs and chargino contributions.

Our paper is organized as follows. In section 2 we review the elements of the MSSM which are relevant for our analysis. In section 3 we give the list of all  $F_r$  functions which can be decomposed into W, charged-Higgs and chargino contributions

$$F_r = (F_r)_{SM} + (F_r)_H + (F_r)_\chi \equiv (F_r)_{SM} + (F_r)_{SUSY} , \quad (1.4)$$

and we compare our results with those given in the literature. In section 4 we collect the formulae for  $\varepsilon$ ,  $B_{d,s}^0 - \bar{B}_{d,s}^0$  mixings,  $\varepsilon'/\varepsilon$  and the rare decays in question. In section 5 some general considerations are given. In particular we address the issue of a *universal unitarity triangle* [43] for all models, like the SM and the constrained MSSM, that do not have any new phases beyond the CKM phase and no new operators. In section 6 we discuss constraints on supersymmetric parameters coming from the  $B \rightarrow X_s \gamma$  decay,  $\Delta\varrho$  in the electroweak precision studies and the lower bound on the neutral Higgs mass. The numerical analysis of the formulae of section 4 including the constraints from section 6 is presented in section 7. Finally section 8 contains a summary and conclusions. A list of auxiliary functions is given in the Appendix.

## 2 The Minimal Supersymmetric Standard Model

### 2.1 FCNC Processes and CP Violation in the MSSM

In general, the MSSM contains more than a hundred new parameters with respect to the SM. A large number of these parameters can be a new source of Flavour-Changing Neutral Currents (FCNC) and of CP violation. Phenomenological studies [38, 44-48] have shown that most of these new flavour- and CP-violating parameters are constrained to be very small by the experimental results on FCNC and CP violation. One is then left with the so-called “flavour problem” and “CP problem”, i.e. with the difficulty of explaining the smallness of these new parameters. We do not discuss here the possible solutions to these problems, but rather assume that they have been solved leading to a version of the MSSM where no new flavour- and CP-violating parameters appear (minimal flavour violation). Although this is not a necessary outcome of the solution of the flavour and CP problems, it is certainly a well-defined and interesting scenario that leads to “minimal” modifications of the SM predictions on FCNC and CP violating processes.

### 2.2 The Model

Let us now specify the details of the MSSM with minimal flavour and CP violation. After applying to the superfields those field redefinitions that diagonalize the quark mass matrices  $M_u$  and  $M_d$ , the squark mass matrices read

$$\tilde{M}_u^2 = \begin{pmatrix} \tilde{M}_{\tilde{q}_L}^2 + (M_u)^2 + M_Z^2 \cos 2\beta \alpha_L^{(u)} & (-\mu^* \cot \beta + A_u^\dagger) M_u \\ M_u (-\mu \cot \beta + A_u) & \tilde{M}_{\tilde{u}_R}^2 + (M_u)^2 + M_Z^2 \cos 2\beta \alpha_R^{(u)} \end{pmatrix} \quad (2.1)$$

$$\tilde{M}_d^2 = \begin{pmatrix} V^\dagger \tilde{M}_{\tilde{q}_L}^2 V + (M_d)^2 + M_Z^2 \cos 2\beta \alpha_L^{(d)} & (-\mu^* \tan \beta + A_d^\dagger) M_d \\ M_d (-\mu \tan \beta + A_d) & \tilde{M}_{\tilde{d}_R}^2 + (M_d)^2 + M_Z^2 \cos 2\beta \alpha_R^{(d)} \end{pmatrix} \quad (2.2)$$

where each entry denotes a three-by-three submatrix and where

$$\begin{aligned} \alpha_L^{(u)} &= \frac{1}{2} - \frac{2}{3} \sin^2 \Theta_W & \alpha_R^{(u)} &= \frac{2}{3} \sin^2 \Theta_W \\ \alpha_L^{(d)} &= -\frac{1}{2} + \frac{1}{3} \sin^2 \Theta_W & \alpha_R^{(d)} &= -\frac{1}{3} \sin^2 \Theta_W. \end{aligned} \quad (2.3)$$

The fact that the explicit squark mass matrices in the two left-left sectors are related by the CKM matrix  $V$  is a remnant of  $SU(2)$  gauge symmetry. The  $3 \times 3$  matrices  $\tilde{M}_{\tilde{q}_L}^2$ ,  $\tilde{M}_{\tilde{u}_R}^2$ ,  $\tilde{M}_{\tilde{d}_R}^2$ ,  $A_u$ ,  $A_d$  are a priori unconstrained complex matrices (except for the hermiticity of  $\tilde{M}_{\tilde{q}_L}^2$ ,  $\tilde{M}_{\tilde{u}_R}^2$ ,  $\tilde{M}_{\tilde{d}_R}^2$ ) parameterizing the soft supersymmetry breaking in the squark sector. We also define, as usual,  $\tan \beta = v_2/v_1$ , while  $\mu$  denotes the supersymmetric Higgs mixing parameter.

In the basis chosen, all neutral-current couplings (couplings of neutral gauge bosons, neutral scalars, and neutral higgsinos and gauginos to quarks and squarks) are still diagonal in the sense that they do not mix members of different quark supermultiplets, while the charged current couplings contain the CKM matrix in the same way as in the SM. However, FCNC arise after diagonalization of the squark mass matrices as soon as any one of the eight  $3 \times 3$  submatrices of eqs. (2.1) and (2.2) is nondiagonal, while new CP violation effects are present if they are not real. Furthermore, we can only have  $\tilde{M}_{\tilde{q}_L}^2$  and  $V^\dagger \tilde{M}_{\tilde{q}_L}^2 V$  diagonal at the same time if

$$\tilde{M}_{\tilde{q}_L}^2 = \tilde{m}^2 \mathbf{1}. \quad (2.4)$$

Our assumption of minimal flavour and CP violation is consequently equivalent to real  $\mu$ , real and diagonal  $A_u$ ,  $A_d$ ,  $\tilde{M}_{\tilde{u}_R}^2$ ,  $\tilde{M}_{\tilde{d}_R}^2$ , and  $\tilde{M}_{\tilde{q}_L}^2 = \tilde{m}^2 \mathbf{1}$ .

The elements of  $A_u$ ,  $A_d$  except the one multiplying the top quark mass are further constrained to be very small by requiring that the model does not develop charge- or color-breaking VEVs or potentials unbounded from below [49-51], so that we may neglect them for all squarks but the stops. Similarly, if  $\tan \beta$  is not too large, the off-diagonal terms proportional to  $\mu$  are negligible for  $\tilde{q} \neq \tilde{t}$ . In this case, the squark mass matrices are already diagonal except for mixing in the stop sector. The real, symmetric stop mass matrix is diagonalized via the orthogonal transformation

$$T \tilde{M}_t^2 T^T = \begin{pmatrix} \tilde{m}_{t_1}^2 & 0 \\ 0 & \tilde{m}_{t_2}^2 \end{pmatrix}, \quad T = \begin{pmatrix} \cos \theta_{\tilde{t}} & \sin \theta_{\tilde{t}} \\ -\sin \theta_{\tilde{t}} & \cos \theta_{\tilde{t}} \end{pmatrix}. \quad (2.5)$$

As a further simplifying assumption, we will set all other squark masses equal, which then implies  $\tilde{m}_{i_L, i_R}^2 \approx \tilde{m}^2$  for  $i = u, d, s, c, b$ . A strict equality is inconsistent with (2.1) and (2.2) for the “left-handed” squarks because of the different D-terms in the up and down sectors, but this difference is numerically insignificant and will be ignored here. We therefore set

$$\tilde{m}_{i_L, i_R}^2 = \tilde{m}^2, \quad i = u, d, s, c, b. \quad (2.6)$$

We then take the input parameters in the squark sector to be the two stop masses and the stop mixing angle  $\theta_{\tilde{t}}$ . From the above we also have

$$\tilde{m}^2 = -m_t^2 + \tilde{m}_{t_1}^2 \cos^2 \theta_{\tilde{t}} + \tilde{m}_{t_2}^2 \sin^2 \theta_{\tilde{t}} \quad (2.7)$$

as a formula for computing  $\tilde{m}$ . We choose  $\tilde{t}_2$  to be the light stop.

In the leptonic sector we neglect Left-Right mixing, and assume, analogously to (2.4) and (2.6),

$$\tilde{m}_{i_L}^2 = \tilde{m}_\ell^2, \quad i = \nu, e. \quad (2.8)$$

The chargino mass matrix is diagonalized by two orthogonal  $2 \times 2$  matrices  $\tilde{U}$  and  $\tilde{V}$ , according to:

$$\tilde{U} \begin{pmatrix} M & m_w \sqrt{2} \sin \beta \\ m_w \sqrt{2} \cos \beta & \mu \end{pmatrix} \tilde{V}^T = \begin{pmatrix} \tilde{m}_{\chi_1} & 0 \\ 0 & \tilde{m}_{\chi_2} \end{pmatrix}, \quad (2.9)$$

where  $\mu$  and  $\tan \beta$  have been introduced before and  $M$  is the weak gaugino mass.  $M$  and  $\mu$  are taken to be real to avoid the appearance of new sources of CP violation. We prefer to choose the lightest chargino mass, which we call  $m_{\chi_1}$ , as an input parameter instead of  $M$ .

In the Higgs sector, the only additional relevant parameter is the mass of the charged Higgs,  $m_{H^\pm}$ .

Altogether, we are left with the seven input parameters  $m_{\tilde{t}_1}$ ,  $m_{\tilde{t}_2}$ ,  $\theta_{\tilde{t}}$ ,  $m_{\chi_1}$ ,  $\mu$ ,  $\tan \beta$ , and  $m_{H^\pm}$ . The ranges for these parameters used in our numerical analysis are discussed in section 7.2. In the computation of the rare decays  $K^+ \rightarrow \pi^+ \nu \bar{\nu}$ ,  $K_L \rightarrow \pi^0 \nu \bar{\nu}$ ,  $K_L \rightarrow \pi^0 e^+ e^-$ ,  $B \rightarrow X_s \nu \bar{\nu}$  and  $B_s \rightarrow \mu \bar{\mu}$  one more input is needed, the slepton mass  $m_{\tilde{\ell}}$ .

## 2.3 Chargino Interactions

Let us denote by  $d$  the quarks ( $d, s, b$ ) and by  $\tilde{u}_k$  the squarks ( $\tilde{u}, \tilde{c}, \tilde{t}$ ) with  $k = 1, 2$ . The interaction of charginos ( $\tilde{\chi}_j^+$ ,  $j = 1, 2$ ) with  $d$  and  $\tilde{u}_k$  is then given explicitly as follows:

$$\mathcal{L}_\chi = g V_{ud}^* \bar{d} (Z_{jk} P_L + Y_{jk} P_R) C \left( \tilde{\chi}_j^+ \right)^T \tilde{u}_k + \text{h.c.} \quad (2.10)$$

where  $P_{L,R} = (1 \mp \gamma_5)/2$ , while  $C$  is the charge conjugation matrix. The couplings  $Z_{jk}$  and  $Y_{jk}$  are real so that the only phases are present in the CKM elements. We have:

$$Y_{j1} = \frac{m_u}{\sqrt{2} M_W \sin \beta} \tilde{V}_{j2} \sin \theta_{\tilde{u}} - \tilde{V}_{j1} \cos \theta_{\tilde{u}} \quad (2.11)$$

$$Y_{j2} = \frac{m_u}{\sqrt{2} M_W \sin \beta} \tilde{V}_{j2} \cos \theta_{\tilde{u}} + \tilde{V}_{j1} \sin \theta_{\tilde{u}} \quad (2.12)$$

$$Z_{j1} = \frac{m_d}{\sqrt{2} M_W \cos \beta} \tilde{U}_{j2} \cos \theta_{\tilde{u}} = 0 \quad (2.13)$$

$$Z_{j2} = -\frac{m_d}{\sqrt{2} M_W \cos \beta} \tilde{U}_{j2} \sin \theta_{\tilde{u}} = 0 \quad (2.14)$$

with  $\tilde{V}_{ji}$  and  $\tilde{U}_{ji}$  defined in (2.9). The  $m_u$  denotes generally the mass of the up-quark ( $u, c, t$ ) corresponding to a given up-squark  $\tilde{u}$ .  $\theta_{\tilde{u}}$  are the mixing angles in the squark sector. Note that since we neglect quark masses other than that of the top, we have  $\theta_{\tilde{u}} = 0$  for  $\tilde{u} \neq \tilde{t}$  (see the preceding section) as well as  $Z_{jk} = 0$ . An exception is the  $B \rightarrow X_s \gamma$  decay in which  $m_b$  and consequently also  $Z_{jk}$  cannot be set to zero.



The Lagrangian (2.10) applies also to lepton-sneutrino-chargino interactions after the CKM factor has been removed and  $\theta_{\tilde{u}}$ ,  $Y_{j2}$  and  $Z_{jk}$  all set to zero. If the masses of charged leptons are neglected only the couplings  $Y_{j1} = -\tilde{V}_{j1}$  are non-vanishing in this case.

Similarly the interaction of charginos with  $u$  and  $\tilde{d}_k$  is given by

$$\mathcal{L}_\chi = gV_{ud}\bar{u} \left( \bar{Z}_{jk}P_L + \bar{Y}_{jk}P_R \right) \tilde{\chi}_j^+ \tilde{d}_k + \text{h.c.} \quad (2.15)$$

where

$$\bar{Y}_{j1} = -\tilde{U}_{j1} \quad (2.16)$$

$$\bar{Y}_{j2} = \bar{Z}_{j1} = \bar{Z}_{j2} = 0. \quad (2.17)$$

The Lagrangian (2.15) describes, mutatis mutandis, the neutrino-slepton-chargino interactions once the CKM factor has been removed.

### 3 Basic Functions

We list next the basic functions which enter the formulae for  $\varepsilon$ ,  $B^0 - \bar{B}^0$  mixing,  $\varepsilon'/\varepsilon$  and rare decays in section 4. The functions relevant for  $\varepsilon$  and  $B^0 - \bar{B}^0$  mixing are given as follows:

$$\begin{aligned} S_{SM}(c, t) &= S(x_{cW}, x_{tW}) \\ S_H(c, t) &= \frac{x_{HW}}{4 \tan^4 \beta} L_2(x_{cH}, x_{tH}, 1) + \frac{2}{\tan^2 \beta} \left[ \frac{1}{4} L_2(x_{cW}, x_{tW}, x_{HW}) - L_1(x_{cW}, x_{tW}, x_{HW}) \right] \\ S_\chi(t, t) &= f(t, t) + f(c, c) - 2f(t, c) \\ f(c, t) &= \sum_{\substack{i,j=1,2 \\ h,k=1,2}} x_{W\chi_j} Y_{i\tilde{c}_h} Y_{i\tilde{t}_k} Y_{j\tilde{c}_h} Y_{j\tilde{t}_k} L_3(x_{\tilde{t}_k\chi_j}, x_{\tilde{c}_h\chi_j}, x_{\chi_i\chi_j}) \end{aligned} \quad (3.18)$$

where  $x_{ab} \equiv m_a^2/m_b^2$ . The functions  $S$  and  $L_{1,2,3}$  are given in the appendix. These results agree with [44, 52, 53]. They agree also with [37] after the erratum has been taken into account.

The functions which include the contributions from photon-penguins ( $D$ ), Z-penguins ( $C$ ), boxes with external  $d\bar{d}$  ( $B^{(d)}$ ),  $u\bar{u}$  ( $B^{(u)}$ ),  $\nu\bar{\nu}$  ( $B^{(\nu\bar{\nu})}$ ),  $e\bar{e}$  ( $B^{(e\bar{e})}$ ) and gluon-penguins ( $E$ ), are given as follows:

$$D = D_{SM}(x_{tW}) + \frac{1}{\tan^2 \beta} D_H(x_{tH}) + 2 \sum_{\substack{j=1,2 \\ k=1,2}} \left[ Y_{j\tilde{t}_k}^2 x_{W\tilde{t}_k} D_\chi(x_{\chi_j\tilde{t}_k}) - (\tilde{t} \rightarrow \tilde{c}) \right] \quad (3.19)$$

$$\begin{aligned} C &= C_{SM}(x_{tW}) + \frac{x_{tW}}{\tan^2 \beta} C_H(x_{tH}) + 2 \sum_{\substack{i,j=1,2 \\ h,k=1,2}} \left[ Y_{j\tilde{t}_k} Y_{i\tilde{t}_h} \left\{ \delta_{ij} \Delta_{hk}^{\tilde{t}} C_\chi^{(1)}(x_{\tilde{t}_h\chi_j}, x_{\tilde{t}_k\chi_j}) \right. \right. \\ &+ \delta_{hk} \left[ \tilde{U}_{i1} \tilde{U}_{j1} C_\chi^{(2)}(x_{\chi_j\tilde{t}_k}, x_{\chi_i\tilde{t}_k}) - \tilde{V}_{i1} \tilde{V}_{j1} C_\chi^{(1)}(x_{\chi_j\tilde{t}_k}, x_{\chi_i\tilde{t}_k}) \right] \left. \right\} - (\tilde{t} \rightarrow \tilde{c}) \Big] \\ &+ \frac{1}{8} \left[ \log x_{\tilde{t}_1\tilde{c}_1} + \sin^2 \theta_{\tilde{t}} \log x_{\tilde{t}_2\tilde{t}_1} \right] \end{aligned} \quad (3.20)$$

where

$$\Delta_{hk}^{\tilde{t}} = \begin{cases} \cos^2 \theta_{\tilde{t}} & k = h = 1 \\ -\sin \theta_{\tilde{t}} \cos \theta_{\tilde{t}} & k \neq h \\ \sin^2 \theta_{\tilde{t}} & k = h = 2 \end{cases} \quad (3.21)$$

$$B^{(d)} = B_{SM}(x_{tw}) + \frac{1}{4} \sum_{\substack{i,j=1,2 \\ k=1,2}} \tilde{V}_{j1} \tilde{V}_{i1} x_{w\chi_j} \left[ Y_{j\tilde{t}_k} Y_{i\tilde{t}_k} B_{\chi}^{(d)}(x_{\tilde{t}_k\chi_j}, x_{\tilde{u}_1\chi_j}, x_{\chi_i\chi_j}) \right. \\ \left. - (\tilde{t} \rightarrow \tilde{c}) \right] \quad (3.22)$$

$$B^{(u)} = B_{SM}(x_{tw}) + \frac{1}{8} \sum_{\substack{i,j=1,2 \\ k=1,2}} \tilde{U}_{j1} \tilde{U}_{i1} x_{w\chi_j} \sqrt{x_{\chi_i\chi_j}} \left[ Y_{j\tilde{t}_k} Y_{i\tilde{t}_k} B_{\chi}^{(u)}(x_{\tilde{t}_k\chi_j}, x_{\tilde{d}_1\chi_j}, x_{\chi_i\chi_j}) \right. \\ \left. - (\tilde{t} \rightarrow \tilde{c}) \right] \quad (3.23)$$

$$B^{(\nu\bar{\nu})} = B_{SM}(x_{tw}) + \frac{1}{8} \sum_{\substack{i,j=1,2 \\ k=1,2}} \tilde{U}_{j1} \tilde{U}_{i1} x_{w\chi_j} \sqrt{x_{\chi_i\chi_j}} \left[ Y_{j\tilde{t}_k} Y_{i\tilde{t}_k} B_{\chi}^{(u)}(x_{\tilde{t}_k\chi_j}, x_{\tilde{e}_1\chi_j}, x_{\chi_i\chi_j}) \right. \\ \left. - (\tilde{t} \rightarrow \tilde{c}) \right] \quad (3.24)$$

$$B^{(e\bar{e})} = B_{SM}(x_{tw}) + \frac{1}{4} \sum_{\substack{i,j=1,2 \\ k=1,2}} \tilde{V}_{j1} \tilde{V}_{i1} x_{w\chi_j} \left[ Y_{j\tilde{t}_k} Y_{i\tilde{t}_k} B_{\chi}^{(d)}(x_{\tilde{t}_k\chi_j}, x_{\tilde{\nu}\chi_j}, x_{\chi_i\chi_j}) \right. \\ \left. - (\tilde{t} \rightarrow \tilde{c}) \right] \quad (3.25)$$

$$E = E_{SM}(x_{tw}) + \frac{1}{\tan^2 \beta} E_H(x_{tH}) + 2 \sum_{\substack{j=1,2 \\ k=1,2}} \left[ Y_{j\tilde{t}_k}^2 x_{w\tilde{t}_k} E_{\chi}(x_{\chi_j\tilde{t}_k}) - (\tilde{t} \rightarrow \tilde{c}) \right] \quad (3.26)$$

The results for the SM and charged Higgs contributions are the same as in [52] and agree with most papers in the literature. The chargino contribution to the  $D$  function given here agrees with [44, 54] and also with the erratum in [37]. Our result for the chargino contribution to the  $C$  function agrees with [44, 54] and the erratum in [37]. The  $C$  functions given in these papers at first sight seem to differ from each other and from our result (3.20). However, after the summations over  $i, j, h, k$  have been performed and the  $\tilde{c}$  part subtracted, the results of these papers reduce to our result. In particular the constant terms in [54] disappear. Note that the convention for  $\theta_{\tilde{t}}$  in [54] differs from ours by a sign.

Next our chargino contribution to  $B^{(d)}$  differs from the result of [37] by an overall sign, while we find the chargino contribution to  $B^{(u)}$  to be a factor of 2 larger than given in the latter paper. Finally our result for the chargino contribution to  $B^{(e\bar{e})}$  agrees with [54] and differs by an overall sign from [44]. In view of the fact that these box contributions are small these differences are unimportant for the whole analysis.

## 4 Compendium of Phenomenological Formulae

### 4.1 Basic Formula for $\varepsilon$

The indirect CP violation in  $K \rightarrow \pi\pi$  is described by the well known parameter  $\varepsilon$ . The general formula for  $\varepsilon$  is given as follows

$$\varepsilon = \frac{\exp(i\pi/4)}{\sqrt{2}\Delta M_K} (\text{Im}M_{12} + 2\xi\text{Re}M_{12}) \quad (4.1)$$

where

$$\xi = \frac{\text{Im}A_0}{\text{Re}A_0} \quad (4.2)$$

with  $A_0 \equiv A(K \rightarrow (\pi\pi)_{I=0})$  and  $\Delta M_K$  being the  $K_L$ - $K_S$  mass difference. The off-diagonal element  $M_{12}$  in the neutral  $K$ -meson mass matrix represents the  $K^0$ - $\bar{K}^0$  mixing. It is given in the MSSM by

$$M_{12} = \frac{G_F^2}{12\pi^2} F_K^2 \hat{B}_K m_K M_W^2 \left[ \lambda_c^{*2} \eta_1 F_{cc} + \lambda_t^{*2} \eta_2 F_{tt} + 2\lambda_c^* \lambda_t^* \eta_3 F_{ct} \right] \quad (4.3)$$

where  $\lambda_i = V_{is}^* V_{id}$  and

$$F_{cc} = S_{SM}(c, c) = x_{cW} \quad (4.4)$$

$$F_{tt} = S_{SM}(t, t) + S_H(t, t) + S_\chi(t, t) \quad (4.5)$$

$$F_{ct} = S_{SM}(c, t) + \frac{\eta_3^H}{\eta_3} S_H(c, t) . \quad (4.6)$$

In what follows we neglect the charged Higgs contribution to  $F_{cc}$ . Due to the assumed mass degeneracy for squarks in the first two generations, chargino exchanges contribute only to  $F_{tt}$ . In what follows we will use the NLO results of [55, 56] for the QCD factors  $\eta_i$ :

$$\eta_1 = 1.38 \quad \eta_2 = 0.57 \quad \eta_3 = 0.47 . \quad (4.7)$$

as obtained in the SM. It should be stressed that in the leading logarithmic approximation (LO)  $\eta_2$  is indeed the same for all three contributions in (4.5). At NLO however this is no longer true because then also gluon corrections to various box diagrams have to be included and these are different for the three contributions in (4.5). These corrections are unknown at present. Since in the SM the NLO corrections to  $\eta_2$  mainly remove the renormalization scale ambiguities present in NLO, we think that in view of other uncertainties in the supersymmetry sector this procedure of using  $\eta_2$  at NLO is justified. In the case of  $F_{ct}$  the QCD corrections to charged Higgs exchanges differ from the SM results already in the leading order and are given by  $\eta_3^H = 0.21$  [52].

Finally  $\hat{B}_K$  is a well known non-perturbative parameter,  $F_K$  is the  $K$ -meson decay constant and  $m_K$  the  $K$ -meson mass. The last term in (4.1) constitutes at most a 2% correction to  $\varepsilon$  and consequently can be neglected in view of other uncertainties, in particular those connected with  $\hat{B}_K$ .

## 4.2 Basic Formula for $B^0 - \bar{B}^0$ Mixing

The  $B^0 - \bar{B}^0$  mixing is usually described by  $(\Delta M)_{d,s}$ , the mass difference between the mass eigenstates in the  $B_d^0 - \bar{B}_d^0$  system and the  $B_s^0 - \bar{B}_s^0$  system, respectively.  $(\Delta M)_{d,s}$  is given as follows:

$$(\Delta M)_{d,s} = \frac{G_F^2}{6\pi^2} \eta_B m_{B_{d,s}} (\hat{B}_{B_{d,s}} F_{B_{d,s}}^2) M_W^2 F_{tt} |V_{t(d,s)}|^2 \quad (4.8)$$

where  $F_{tt}$  is again the function given in (4.5).  $\hat{B}_B$  is a non-perturbative parameter analogous to  $\hat{B}_K$ ,  $F_B$  is the B-decay constant and  $\eta_B$  the QCD factor given at NLO in the SM by  $\eta_B = 0.55$  [55, 57]. Supersymmetric corrections modify this factor first at the NLO level. As they are unknown at present we will use the SM value for  $\eta_B$  also in the MSSM.

## 4.3 Basic Formula for $\varepsilon'/\varepsilon$

Using the functions listed in Section 3, the formula for  $\varepsilon'/\varepsilon$  of [5] generalizes to the supersymmetric case as follows:

$$\frac{\varepsilon'}{\varepsilon} = \text{Im} \lambda_t \cdot F_{\varepsilon'} \quad (4.9)$$

where

$$F_{\varepsilon'} = P_0 + P_X X + P_Y Y + P_Z Z + P_E E \quad (4.10)$$

with

$$X = C - 4B^{(u)}, \quad Y = C - B^{(d)}, \quad Z = C + \frac{1}{4}D. \quad (4.11)$$

The functions  $D$ ,  $C$ ,  $B^{(d)}$ ,  $B^{(u)}$  and  $E$  are listed in (3.19)–(3.26). Retaining only the SM contributions in the latter functions one obtains the formula (2.38) of [5].

The coefficients  $P_i$  are given in terms of the non-perturbative parameters  $B_6^{(1/2)}$  and  $B_8^{(3/2)}$  and the strange quark mass  $m_s(m_c)$  as follows:

$$P_i = r_i^{(0)} + r_i^{(6)} R_6 + r_i^{(8)} R_8 \quad (4.12)$$

where

$$R_6 \equiv B_6^{(1/2)} \left[ \frac{137 \text{ MeV}}{m_s(m_c) + m_d(m_c)} \right]^2, \quad R_8 \equiv B_8^{(3/2)} \left[ \frac{137 \text{ MeV}}{m_s(m_c) + m_d(m_c)} \right]^2. \quad (4.13)$$

	$\Lambda_{\overline{\text{MS}}}^{(4)} = 290 \text{ MeV}$			$\Lambda_{\overline{\text{MS}}}^{(4)} = 340 \text{ MeV}$			$\Lambda_{\overline{\text{MS}}}^{(4)} = 390 \text{ MeV}$		
$i$	$r_i^{(0)}$	$r_i^{(6)}$	$r_i^{(8)}$	$r_i^{(0)}$	$r_i^{(6)}$	$r_i^{(8)}$	$r_i^{(0)}$	$r_i^{(6)}$	$r_i^{(8)}$
0	-3.122	10.905	1.423	-3.167	12.409	1.262	-3.210	14.152	1.076
$X$	0.556	0.019	0	0.540	0.023	0	0.526	0.027	0
$Y$	0.404	0.080	0	0.387	0.088	0	0.371	0.097	0
$Z$	0.412	-0.015	-9.363	0.474	-0.017	-10.186	0.542	-0.019	-11.115
$E$	0.204	-1.276	0.409	0.188	-1.399	0.459	0.172	-1.533	0.515
0	-3.097	9.586	1.045	-3.141	10.748	0.867	-3.183	12.058	0.666

Table 2: Coefficients in the formula (4.12) for various  $\Lambda_{\overline{\text{MS}}}^{(4)}$  in the NDR scheme. The last row gives the  $r_0$  coefficients in the HV scheme.

$B_6^{(1/2)}$  and  $B_8^{(3/2)}$  parameterize the matrix elements of the dominant QCD-penguin ( $Q_6$ ) and the dominant electroweak penguin ( $Q_8$ ) operator respectively. The numerical values of  $r_i^{(0)}$ ,  $r_i^{(6)}$  and  $r_i^{(8)}$  for different values of  $\Lambda_{\overline{\text{MS}}}^{(4)}$  at  $\mu = m_c$  in the NDR renormalization scheme are given in table 2. This table differs from the one presented in [5] in that  $\Omega_{\eta+\eta'} = 0.25$  has been replaced by  $\Omega_{\eta+\eta'} = 0.16$  in accordance with the most recent calculation in [58] which gives  $\Omega_{\eta+\eta'} = 0.16 \pm 0.03$  (see however [26]). All other input parameters are as in [5] where further details connected with the coefficients in (4.12) and the parameters  $B_6^{(1/2)}$  and  $B_8^{(3/2)}$  can be found.

#### 4.4 Rare K and B Decays

The well known expressions for rare K and B decays in the SM can easily be generalized to the corresponding expressions in the MSSM. We have [24]

$$Br(K^+ \rightarrow \pi^+ \nu \bar{\nu}) = 1.54 \cdot 10^{-4} \cdot \left[ \left( \text{Im} \lambda_t \cdot X^{(\nu \bar{\nu})} \right)^2 + \left( \text{Re} \lambda_c \cdot \bar{X}_c + \text{Re} \lambda_t \cdot X^{(\nu \bar{\nu})} \right)^2 \right], \quad (4.14)$$

where  $\bar{X}_c = (9.8 \pm 1.4) \cdot 10^{-4}$  stands for the internal charm contribution evaluated at NLO in the SM [59].  $\text{Re} \lambda_c = -\lambda(1 - \lambda^2/2)$  with  $\lambda = 0.22$ . The supersymmetric contributions reside only in  $X^{(\nu \bar{\nu})}$ .

$$Br(K_L \rightarrow \pi^0 \nu \bar{\nu}) = 6.8 \cdot 10^{-4} \cdot \left( \text{Im} \lambda_t \cdot X^{(\nu \bar{\nu})} \right)^2 \quad (4.15)$$

$$Br(K_L \rightarrow \pi^0 e^+ e^-)_{\text{dir}} = 6.3 \cdot 10^{-6} (\text{Im} \lambda_t)^2 (\tilde{g}_{7A}^2 + \tilde{g}_{7V}^2), \quad (4.16)$$

where

$$\tilde{y}_{7V} = P_0 + \frac{Y^{(e\bar{e})}}{\sin^2 \Theta_W} - 4Z, \quad \tilde{y}_{7A} = -\frac{1}{\sin^2 \Theta_W} Y^{(e\bar{e})} \quad (4.17)$$

with  $P_0 = 3.05 \pm 0.08$  including NLO corrections [60] and  $\sin^2 \Theta_W = 0.23$ . In (4.16) we have only given the directly CP violating contribution to this decay.

Finally

$$Br(B \rightarrow X_s \nu \bar{\nu}) = 1.5 \cdot 10^{-5} \frac{|V_{ts}|^2}{|V_{cb}|^2} \left( X^{(\nu\bar{\nu})} \right)^2, \quad (4.18)$$

$$Br(B_s \rightarrow \mu^+ \mu^-) = 3.3 \cdot 10^{-9} \left[ \frac{\tau(B_s)}{1.6\text{ps}} \right] \left[ \frac{F_{B_s}}{210\text{MeV}} \right]^2 \left[ \frac{|V_{ts}|}{0.040} \right]^2 \left( Y^{(e\bar{e})} \right)^2 \quad (4.19)$$

where  $\tau(B_s)$  and  $F_{B_s}$  is the life-time and the decay constant of the  $B_s$  meson respectively.

The functions  $X^{(\nu\bar{\nu})}$  and  $Y^{(e\bar{e})}$  are given as follows

$$X^{(\nu\bar{\nu})} = C - 4B^{(\nu\bar{\nu})}, \quad Y^{(e\bar{e})} = C - B^{(e\bar{e})}. \quad (4.20)$$

with  $C$ ,  $B^{(\nu\bar{\nu})}$ ,  $B^{(e\bar{e})}$  listed in (3.20), (3.24) and (3.25) respectively. The function  $Z$  is defined in (4.11).

## 5 General Considerations

### 5.1 Strategy A: Universal Unitarity Triangle

The SM, the MSSM and any model in which all flavour changing transitions are governed by the CKM matrix with no new phases beyond the CKM one and no new local operators beyond those present in the SM, share a useful property [43]. Namely, the CKM parameters in these models extracted from a particular set of data are independent of the basic functions of section 3, they are universal in this class of models. Correspondingly there exists a *universal unitarity triangle*. In particular a determination of CKM parameters and of this universal unitarity triangle without the knowledge of supersymmetric parameters is possible.

Indeed using (4.8) one finds

$$\frac{|V_{td}|}{|V_{ts}|} = \xi \sqrt{\frac{m_{B_s}}{m_{B_d}}} \sqrt{\frac{(\Delta M)_d}{(\Delta M)_s}} \equiv \kappa, \quad \xi = \frac{F_{B_s} \sqrt{\hat{B}_{B_s}}}{F_{B_d} \sqrt{\hat{B}_{B_d}}}. \quad (5.1)$$

That is the ratio  $\kappa$  depends only on the measurable quantities  $(\Delta M)_{d,s}$ ,  $m_{B_{d,s}}$  and the non-perturbative parameter  $\xi$ . Now to an excellent accuracy [61]:

$$|V_{td}| = |V_{cb}| \lambda R_t, \quad R_t = \sqrt{(1 - \bar{\varrho})^2 + \bar{\eta}^2} \quad (5.2)$$

$$|V_{ts}| = |V_{cb}|(1 - \frac{1}{2}\lambda^2 + \bar{\varrho}\lambda^2) \quad (5.3)$$

where

$$\bar{\varrho} = \varrho(1 - \frac{1}{2}\lambda^2), \quad \bar{\eta} = \eta(1 - \frac{1}{2}\lambda^2) \quad (5.4)$$

with  $\lambda = 0.22$ ,  $\varrho$  and  $\eta$  being Wolfenstein parameters. We note next that through unitarity of the CKM matrix and the present lower bound on  $(\Delta M)_s$  one has both in the SM and in the MSSM  $0 \leq \bar{\varrho} \leq 0.5$ . Consequently  $|V_{ts}|$  deviates from  $|V_{cb}|$  by at most 2.5%. This means that to a very good accuracy the length of one side of the unitarity triangle is given by

$$R_t = \frac{\kappa}{\lambda} \quad (5.5)$$

independently of supersymmetric parameters and  $m_t$ . In order to complete the determination of  $\bar{\varrho}$  and  $\bar{\eta}$  one can use  $\sin 2\beta$  extracted either from the CP asymmetry in  $B_d \rightarrow \psi K_S$  or from  $K \rightarrow \pi\nu\bar{\nu}$  decays [62]. Both extractions are independent to an excellent accuracy of the supersymmetric parameters and  $m_t$ . Once  $R_t$  and  $\sin 2\beta$  have been determined in this manner,  $\bar{\varrho}$  and  $\bar{\eta}$  can be found through [43, 63]

$$\bar{\eta} = \frac{R_t}{\sqrt{2}} \sqrt{\sin 2\beta \cdot r_-(\sin 2\beta)}, \quad \bar{\varrho} = 1 - \bar{\eta} r_+(\sin 2\beta) \quad (5.6)$$

where  $r_{\pm}(z) = (1 \pm \sqrt{1 - z^2})/z$ . In general the calculation of  $\bar{\varrho}$  and  $\bar{\eta}$  from  $R_t$  and  $\sin 2\beta$  involves discrete ambiguities. As described in [43, 63] they can be resolved by using further information, for instance coming from  $|V_{ub}/V_{cb}|$  and  $\varepsilon$ , so that eventually the solution (5.6) is singled out.

As an alternative to  $\sin 2\beta$  one could use the measurement of  $\sqrt{\bar{\varrho}^2 + \bar{\eta}^2}$  by means of  $|V_{ub}/V_{cb}|$  but this strategy suffers from hadronic uncertainties in the extraction of  $|V_{ub}/V_{cb}|$ .

We observe that provided  $(\Delta M)_s$  has been measured and  $\sin 2\beta$  extracted from CP asymmetry in  $B_d \rightarrow \psi K_S$  or  $K \rightarrow \pi\nu\bar{\nu}$  one can determine the “true” values of  $\bar{\eta}$  and  $\bar{\varrho}$  independently of supersymmetric parameters. Since  $\lambda$  and  $|V_{cb}| = A\lambda^2$  are determined from tree level K and B decays they are insensitive to new physics as well. Thus the full CKM matrix can be determined in this manner. The corresponding universal unitarity triangle common to the SM and the restricted MSSM can be found directly from (5.6).

Having the universal values of  $\bar{\varrho}$  and  $\bar{\eta}$  at hand one can calculate  $\varepsilon$ ,  $\varepsilon'/\varepsilon$ ,  $(\Delta M)_d$ ,  $(\Delta M)_s$  and branching ratios for rare decays. As these quantities depend on supersymmetric parameters the results for the SM and the MSSM will generally differ from each other and one will be able to find out whether the SM or the MSSM, if any of these two models, is singled out by the data. In our opinion the use of the universal unitarity triangle is the most transparent strategy for distinction between models belonging to this class. It will certainly play an important role once  $(\Delta M)_s$  has been measured and  $\sin 2\beta$  extracted

either from the CP asymmetry in  $B_d^0 \rightarrow \psi K_S$  or from  $K \rightarrow \pi \nu \bar{\nu}$  decays. Other strategies for the determination of the universal unitarity triangle are discussed in [43].

## 5.2 Strategy B: Present

As  $(\Delta M)_s$  and  $\sin 2\beta$  from  $B_d \rightarrow \psi K_S$  or  $K \rightarrow \pi \nu \bar{\nu}$  are presently not available we do not know the “true” values of the CKM parameters. However, by fitting theoretical expressions for  $\varepsilon$  and  $(\Delta M)_d$  to the experimental data we can find out for which values of CKM parameters the SM and the MSSM reproduce these data. As this determination involves the basic functions of section 3, the resulting values of CKM parameters in the MSSM will generally differ from the corresponding values in the SM. This difference has to be taken into account when making predictions for  $\varepsilon'/\varepsilon$  and rare decays branching ratios.

A different strategy has been adopted in [64]. These authors have assumed all CKM parameters in the MSSM to be equal to those in the SM. This would be a correct strategy if we knew the universal triangle but in its absence it could be misleading. Indeed as a result of this assumption  $(\Delta M)_d^{\text{MSSM}}$  in [64] can differ from  $(\Delta M)_d^{\text{SM}}$  by as much as 20% which is well outside the experimental error for  $(\Delta M)_d$  that amounts to  $\pm 3\%$ . The same comment applies to the parameter  $\varepsilon$  where the experimental error is even smaller. This means that either the SM or the MSSM is already ruled out which of course is not true at present.

In our opinion the only correct procedure at present is to impose the conditions

$$(\Delta M)_d^{\text{SM}} = (\Delta M)_d^{\text{MSSM}} = (\Delta M)_d^{\text{exp}} , \quad (\varepsilon)^{\text{SM}} = (\varepsilon)^{\text{MSSM}} = (\varepsilon)^{\text{exp}} . \quad (5.7)$$

As this conditions are used in our paper, our results for the rare decays branching ratios differ from the ones in [64].

Now, from  $(\Delta M)_d^{\text{SM}} = (\Delta M)_d^{\text{MSSM}}$  it follows that

$$|V_{td}|_{\text{MSSM}}^2 = |V_{td}|_{\text{SM}}^2 \frac{(F_{tt})_{\text{SM}}}{(F_{tt})_{\text{MSSM}}} \frac{\eta_B^{\text{SM}}}{\eta_B^{\text{MSSM}}} . \quad (5.8)$$

where the last factor takes into account the small difference between QCD factors in the MSSM and the SM which appears at the two-loop level. We will set  $\eta_B^{\text{MSSM}} = \eta_B^{\text{SM}}$  in what follows.

As  $(F_{tt})_{\text{MSSM}} > (F_{tt})_{\text{SM}}$  one has

$$|V_{td}|_{\text{MSSM}}^2 < |V_{td}|_{\text{SM}}^2 . \quad (5.9)$$

Similarly,

$$(\text{Im}\lambda_t)_{\text{MSSM}} < (\text{Im}\lambda_t)_{\text{SM}}, \quad |(\text{Re}\lambda_t)_{\text{MSSM}}| < |(\text{Re}\lambda_t)_{\text{SM}}| \quad (5.10)$$



when the constraints from  $(\Delta M)_d$  and  $\varepsilon$  are imposed. These hierarchies agree with the recent analysis in [65].

On the other hand  $|V_{ts}|$  can only be modified by supersymmetric contributions through the change of  $\bar{\varrho}$  in (5.3). As this is an  $\mathcal{O}(\lambda^2)$  effect and  $0 \leq \bar{\varrho} \leq 0.5$  from unitarity and  $|V_{ub}/V_{cb}|$  we have within 2.5%

$$|V_{ts}|_{\text{MSSM}} = |V_{ts}|_{\text{SM}} = |V_{cb}|. \quad (5.11)$$

These results have the following consequences:

- Quantities sensitive to  $|V_{td}|$ ,  $\text{Im}\lambda_t$  and  $\text{Re}\lambda_t$  experience a suppression in the MSSM relative to the SM through the CKM parameters which may or may not be compensated by the loop effects relevant for a given process. In particular we have:

$$\frac{Br(K_L \rightarrow \pi^0 \nu \bar{\nu})_{\text{MSSM}}}{Br(K_L \rightarrow \pi^0 \nu \bar{\nu})_{\text{SM}}} = \frac{(\text{Im}\lambda_t)_{\text{MSSM}}^2}{(\text{Im}\lambda_t)_{\text{SM}}^2} \left[ \frac{X_{\text{MSSM}}^{\nu\bar{\nu}}}{X_{\text{SM}}^{\nu\bar{\nu}}} \right]^2, \quad (5.12)$$

$$\frac{Br(K_L \rightarrow \pi^0 e^- e^+)_{\text{MSSM}}^{\text{dir}}}{Br(K_L \rightarrow \pi^0 e^- e^+)_{\text{SM}}^{\text{dir}}} = \frac{(\text{Im}\lambda_t)_{\text{MSSM}}^2}{(\text{Im}\lambda_t)_{\text{SM}}^2} \frac{(\tilde{y}_{7A}^2 + \tilde{y}_{7V}^2)_{\text{MSSM}}}{(\tilde{y}_{7A}^2 + \tilde{y}_{7V}^2)_{\text{SM}}}, \quad (5.13)$$

$$\frac{(\varepsilon'/\varepsilon)_{\text{MSSM}}}{(\varepsilon'/\varepsilon)_{\text{SM}}} = \frac{(\text{Im}\lambda_t)_{\text{MSSM}}}{(\text{Im}\lambda_t)_{\text{SM}}} \frac{F_{\varepsilon'}^{\text{MSSM}}}{F_{\varepsilon'}^{\text{SM}}}. \quad (5.14)$$

Moreover in the approximation of neglecting the charm contribution to  $K^+ \rightarrow \pi^+ \nu \bar{\nu}$  one finds using (5.8)

$$\frac{Br(K^+ \rightarrow \pi^+ \nu \bar{\nu})_{\text{MSSM}}}{Br(K^+ \rightarrow \pi^+ \nu \bar{\nu})_{\text{SM}}} = \frac{(F_{tt})_{\text{SM}}}{(F_{tt})_{\text{MSSM}}} \left[ \frac{X_{\text{MSSM}}^{\nu\bar{\nu}}}{X_{\text{SM}}^{\nu\bar{\nu}}} \right]^2. \quad (5.15)$$

Of course, in our numerical analysis we keep the charm contribution.

- Quantities sensitive to  $|V_{ts}|$  depend to a very good approximation on supersymmetric effects only through loop effects relevant for a given process. In particular we have

$$\frac{Br(B \rightarrow X_s \nu \bar{\nu})_{\text{MSSM}}}{Br(B \rightarrow X_s \nu \bar{\nu})_{\text{SM}}} = \left[ \frac{X_{\text{MSSM}}^{\nu\bar{\nu}}}{X_{\text{SM}}^{\nu\bar{\nu}}} \right]^2, \quad (5.16)$$

$$\frac{Br(B_s \rightarrow \mu \bar{\mu})_{\text{MSSM}}}{Br(B_s \rightarrow \mu \bar{\mu})_{\text{SM}}} = \left[ \frac{Y_{\text{MSSM}}^{e\bar{e}}}{Y_{\text{SM}}^{e\bar{e}}} \right]^2. \quad (5.17)$$

- From (5.12) and (5.14) we have

$$\frac{(\varepsilon'/\varepsilon)_{\text{MSSM}}}{(\varepsilon'/\varepsilon)_{\text{SM}}} = \sqrt{\frac{Br(K_L \rightarrow \pi^0 \nu \bar{\nu})_{\text{MSSM}}}{Br(K_L \rightarrow \pi^0 \nu \bar{\nu})_{\text{SM}}} \frac{F_{\varepsilon'}^{\text{MSSM}}}{F_{\varepsilon'}^{\text{SM}}} \frac{X_{\text{SM}}^{\nu\bar{\nu}}}{X_{\text{MSSM}}^{\nu\bar{\nu}}}}. \quad (5.18)$$

These observations should be helpful in understanding the numerical results presented in section 7. It should also be remarked that the formulae (5.12)–(5.18) are also valid for strategy A after the  $\text{Im}\lambda_t$  and  $F_{tt}$  have been removed from these equations.

## 6 Constraints

### 6.1 The $B \rightarrow X_s \gamma$ constraint

The latest data [66] for the inclusive radiative decay rate of the  $B$  meson are known to constrain severely the accessible supersymmetric parameter space (see for instance [67, 68]). This decay mode is controlled by the magnetic penguin operator  $Q_7$ , whose Wilson coefficient at the weak scale can be written as

$$C_{7\gamma}(M_W) = A_{SM}^{(\gamma)} + A_H^{(\gamma)} + A_\chi^{(\gamma)}, \quad (6.19)$$

where  $A_{SM}^{(\gamma)}$ ,  $A_H^{(\gamma)}$ , and  $A_\chi^{(\gamma)}$  are the contributions from  $W$ , charged Higgs, and chargino loops, respectively.

For a light charged Higgs mass,  $A_H^{(\gamma)}$  is large and always adds to the SM contribution, driving the branching ratio towards very high values. Therefore, only large chargino-stop contributions that interfere destructively with the charged Higgs ones can accommodate the present data [69]. On the other hand, unless the charged Higgs is very heavy, this requires the existence of at least one light chargino and one light stop and restricts considerably the allowed SUSY parameter space. In our analysis we therefore include this constraint using the latest theoretical and experimental information.

A complete NLO analysis of  $B \rightarrow X_s \gamma$  is by now available in the SM [70, 71] and in the 2HDM [71, 72]. The references to earlier LO calculations can be found in [24]. As a result of these efforts, the error on the theoretical prediction coming from uncalculated higher orders is estimated to be of the order of 5%, while large parametric uncertainties are induced by the semileptonic BR, used as a normalization, the bottom and charm masses, the CKM factor, and to a lesser extent by the top mass and  $\alpha_s$ . In the case of the SM and of the type II 2HDM the overall theoretical error is generally around 10%. In the numerical analysis we fully implement all the NLO contributions to SM and 2HDM components including the latest refinements [73].

For what concerns the purely supersymmetric contributions, there exist no complete NLO calculation. However, the case considered in the present paper (minimal flavour violation) has been studied in [74, 75], where the Wilson coefficients have been expanded in inverse powers of the gluino and heavy squark masses. This approximation is designed to capture two sources of large NLO effects: i) if large cancellations between charged Higgs and chargino contribution occur at LO, they can be spoiled at NLO ; ii) the existence of large splitting among supersymmetric particles can lead to large *non-decoupling* logarithms.

In our numerical study we employ the results of [74] whenever they are applicable: we define a light mass scale  $M_l$  as the heavier between  $\tilde{m}_{t_2}$ ,  $\tilde{m}_{\chi_1}$ , and a heavy mass scale  $M_h$

as the minimum of  $\tilde{m}_g$ ,  $\tilde{m}_{t_1}$  and  $\tilde{m}$ ; if the condition  $M_h > 2M_l$  is satisfied, the chargino contributions to the Wilson coefficients are evaluated at NLO, otherwise we use the LO expressions. Similarly, we employ the NLO expressions only if  $|\tilde{\theta}_t| < \pi/10$ .

The estimate of the theoretical error is expected to compensate for this different treatment. We adopt a rather conservative approach: we scan over all the unphysical scales, using  $2.4 < \mu_b, \bar{\mu}_b < 9.6$  GeV and  $40 < \mu_W < 160$  GeV (notation of [71]) and combine in quadrature the parametric uncertainties. The two extreme values of the BR obtained combining linearly these two uncertainties are then compared with the CLEO 95% C.L.  $BR_\gamma > 2.0 \times 10^{-4}$  and  $BR_\gamma < 4.5 \times 10^{-4}$ .

## 6.2 Constraints from electroweak precision tests

The good agreement between the SM predictions and the electroweak precision data favours those types of new physics for which contributions decouple from the precision observables. As we also consider light superpartners, we need to take into account the tight constraints on the supersymmetric spectrum emerging from this agreement.

In the case of the MSSM, several recent and thorough analyses are available in the literature [67, 76]. The most relevant effect is due to the mass splitting of the superpartners, and in particular of the third generation squarks. Indeed, large splitting between  $\tilde{m}_{b_L}$  and  $\tilde{m}_{t_L}$  would induce large contributions to the electroweak  $\rho$  parameter of the same sign of the standard quadratic top quark term. This universal contribution enters the  $Z^0$  boson couplings and the relation between  $M_W$ ,  $G_\mu$  and  $\alpha$  and is therefore significantly constrained by present data. Following the assumptions of section 2, the contribution of the squarks to  $\Delta\rho = 1 - 1/\rho$  is given at one-loop order by the simple expression [77, 78]

$$\begin{aligned} \Delta^{\tilde{q}}\rho^{(0)} &= \frac{3G_F}{8\sqrt{2}\pi^2} \left[ -\sin^2\theta_{\tilde{t}} \cos^2\theta_{\tilde{t}} F(m_{\tilde{t}_1}^2, m_{\tilde{t}_2}^2) \right. \\ &\quad \left. + \cos^2\theta_{\tilde{t}} F(m_{\tilde{t}_1}^2, m_{\tilde{b}_L}^2) + \sin^2\theta_{\tilde{t}} F(m_{\tilde{t}_2}^2, m_{\tilde{b}_L}^2) \right], \end{aligned} \quad (6.20)$$

with the function  $F$  given by

$$F(x, y) = x + y - \frac{2xy}{x - y} \log \frac{x}{y}.$$

Notice that  $\Delta^{\tilde{q}}\rho^{(0)}$  in (6.20) vanishes for degenerate squarks and when one of the squarks becomes very heavy it is proportional to the square of its mass. Of course, squark contributions are not the only supersymmetric corrections to  $\Delta\rho$ . However, they are the only potentially large ones, when the present direct exclusion bounds are taken into account, and the other contributions have in general the same sign [78].

In the cases of the  $W$ -boson mass and of the effective weak mixing angle  $\sin^2 \Theta_W^{\text{eff}}$ , for example, a doublet of heavy squarks would induce shifts proportional to its contribution to  $\rho$ ,

$$\delta M_W/M_W \approx 0.72 \Delta\rho; \quad \delta \sin^2 \Theta_W^{\text{eff}} \approx -0.33 \Delta\rho. \quad (6.21)$$

As the relative experimental accuracy for these quantities is  $5 \times 10^{-4}$  and  $7 \times 10^{-4}$ , respectively, it is easy to realize that the present sensitivity to  $\Delta\rho$  is at the level of  $1 \times 10^{-3}$ . Of course, a global fit provides a better way to explore this sensitivity. The model-independent analysis of [79], based on 1998 data, finds a value  $(3.7 \pm 1.1) 10^{-3}$  for the parameter  $\epsilon_1 \approx \Delta\rho$ , where the central value is close to the SM result, but favours smaller values than in the SM. As  $\Delta\rho_{\text{susy}}$  is positive, it is tightly constrained. The analysis of [80], on the other hand, includes also the information relative to the restricted Higgs sector of the MSSM and leads to  $\Delta\rho_{\text{susy}} = -0.0004^{+0.0017}_{-0.0013}$  at the  $2\sigma$  level, which again shows no deviations from the SM. Another alternative formulation in terms of the parameter  $T \approx \alpha\Delta\rho$  leads to very similar results ( $0 < T_{\text{susy}} < 0.2$  at 95% CL [67, 76]). We will therefore require

$$\Delta\tilde{\rho}^{(0)} < 1.5 \times 10^{-3},$$

which appears to be a conservative bound, also taking into account that QCD effects tend to enhance significantly the squark contributions to  $\Delta\rho$  [81], and that present data improve on the 1998 results employed in [79, 80], especially on  $M_W$ .

### 6.3 Direct exclusion bound on $M_h$

The tree level MSSM relation between the mass of the lightest CP-even Higgs boson and  $M_Z$ ,  $M_h \leq M_Z |\cos 2\beta| \leq M_Z$ , is subject to very large radiative corrections (a summary of the most recent results with exhaustive references can be found in [82]), which relax it into a much looser bound  $M_h < 135$  GeV. The precise value of  $M_h$  depends sensitively on the supersymmetric parameters and in particular on  $\tan \beta$ , the mass of the pseudoscalar,  $M_A$  — which at lowest order is linked to the mass of the charged Higgs by  $M_{H^\pm}^2 = M_A^2 + M_W^2$  — and the third generation squarks, which give the most important loop contributions.

At LEP-200 the lightest MSSM neutral Higgs can be produced mainly via the Higgs-strahlung process  $e^+e^- \rightarrow h Z$  and the pair production process  $e^+e^- \rightarrow h A$ . The experimental searches have so far set a lower bound on the mass of the light neutral Higgs of about 88 GeV [83]. As this already excludes large regions of the supersymmetric parameter space, especially if  $\tan \beta$  is low, it is important to include also this constraint in our analysis. To this end we employ approximate formulas based on [84]; unfortunately, they cannot be used for  $M_{tLR} > 2M_{\tilde{q}}$  and do not cover part of our parameter space. Therefore, for  $M_{tLR} > 2M_{\tilde{q}}$  we use the full one-loop expression to compute the Higgs mass

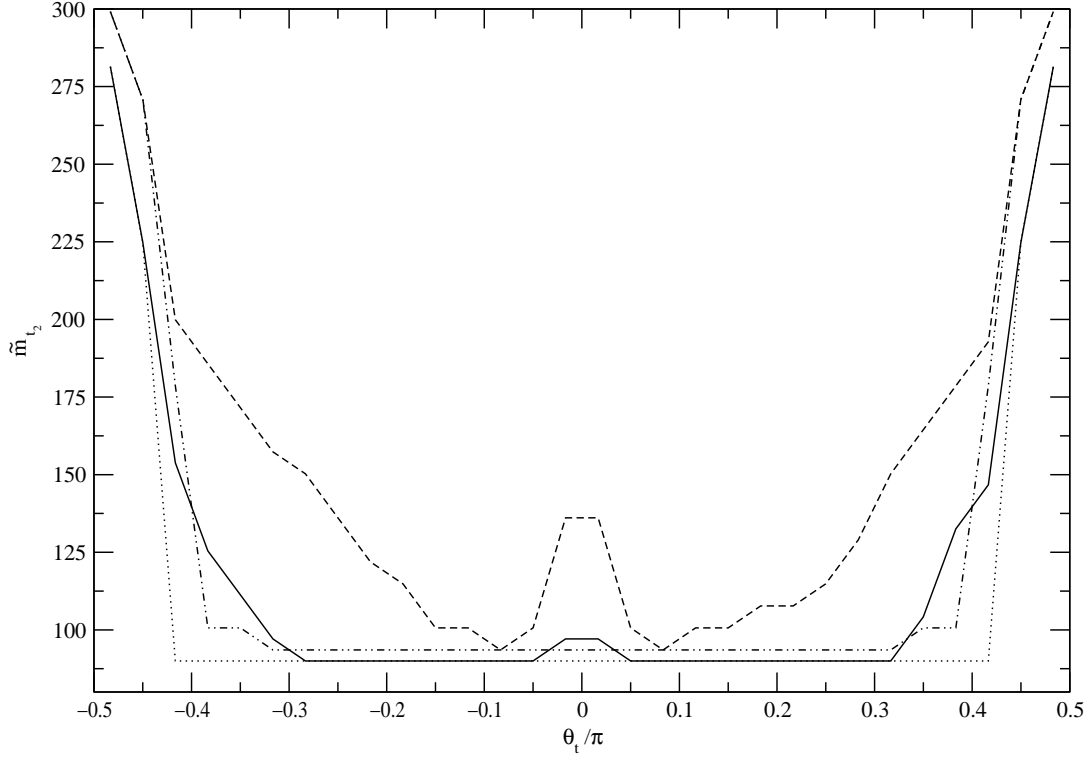


Figure 1: Contour plot in the  $\tilde{m}_{t_2} - \theta_{\tilde{t}}$  plane. The regions above the dash-dotted and dotted lines contain 95% and 100% of the generated points respectively, without taking the constraints discussed in section 6 into account. The regions above the dashed and continuous lines contain 95% and 100% of the allowed points respectively, once the constraints are taken into account.

[85]. We notice that for large splitting between the stop masses new large logarithms enter the analysis which may induce relatively large QCD corrections and may need to be resummed. To the best of our knowledge, this case has not been considered in the literature. However we believe this does not affect our main conclusions.

The relevance of the constraints discussed in this section on the SUSY parameter space can be seen, for example, in fig. 1, where we present the contour plot of the light stop mass versus the stop mixing angle in the ranges described in section 7.2, with and without the constraints discussed above. Clearly, a large portion of the region where one of the stops is very light is excluded by the present constraints.

## 7 Numerical Analysis

### 7.1 Standard Model Parameters

In order to make predictions for  $\varepsilon'/\varepsilon$  and rare decays we need the values of  $\text{Im}\lambda_t$  and  $\text{Re}\lambda_t$ . They can be obtained from the standard analysis of the unitarity triangle which uses the data for  $|V_{cb}|$ ,  $|V_{ub}|$ ,  $\varepsilon$ ,  $(\Delta M)_d$  and  $(\Delta M)_s$ , where the last two measure the size of  $B_{d,s}^0 - \bar{B}_{d,s}^0$  mixings. The relevant formulae for  $\varepsilon$  and  $(\Delta M)_{d,s}$  are given in sections 4.1 and 4.2 respectively. We also recall that the present lower bound on  $(\Delta M)_s$  together with  $(\Delta M)_d$  puts the following constraint on the ratio  $|V_{td}|/|V_{ts}|$ :

$$\frac{|V_{td}|}{|V_{ts}|} < \xi \sqrt{\frac{m_{B_s}}{m_{B_d}}} \sqrt{\frac{(\Delta M)_d}{(\Delta M)_s^{\min}}} \quad (7.1)$$

with the non-perturbative parameter  $\xi$  defined in (5.1). As discussed in section 5 the constraint in (7.1) is valid both in the SM and in the MSSM.

The input parameters needed to perform the analysis of the unitarity triangle within the SM are:

$$|V_{cb}|, \quad |V_{ub}|, \quad m_c, \quad m_t, \quad \hat{B}_K, \quad \sqrt{\hat{B}_d} F_{B_d}, \quad \xi. \quad (7.2)$$

Their values are given in table 3, where  $m_t$  refers to the running current top quark mass defined at  $\mu = m_t^{\text{Pole}}$ . It corresponds to  $m_t^{\text{Pole}} = 174.3 \pm 5.1$  GeV measured by CDF and D0.

It should be emphasized that  $\hat{B}_K$ ,  $\sqrt{\hat{B}_d} F_{B_d}$  and  $\xi$  being obtained from the calculations of hadronic matrix elements in QCD are unaffected by the presence of supersymmetry. The extraction of the remaining parameters in (7.2) from the data could in principle be affected by supersymmetric contributions but at least within MSSM such contributions are safely negligible.

The additional input parameters required to perform the analysis of  $\varepsilon'/\varepsilon$  within the SM are

$$\Lambda_{\overline{\text{MS}}}^{(4)}, \quad m_s(m_c), \quad B_6^{(1/2)}, \quad B_8^{(3/2)} \quad (7.3)$$

Their values are given in table 3, where the values for  $\Lambda_{\overline{\text{MS}}}^{(4)}$  and  $m_s(m_c)$  correspond roughly to  $\alpha_s(M_Z) = 0.119 \pm 0.003$ , and  $m_s(2 \text{ GeV}) = (110 \pm 20) \text{ MeV}$  respectively.

Again the non-perturbative parameters  $B_6^{(1/2)}$  and  $B_8^{(3/2)}$  are unaffected by the presence of supersymmetry. The extraction of  $\Lambda_{\overline{\text{MS}}}^{(4)}$  and  $m_s(m_c)$  from the data could in principle be affected by supersymmetric contributions but at least within the MSSM such contributions are safely negligible.

In summary the values of the input parameters given in table 3 are common to the SM and MSSM. On the other hand the resulting values of  $\text{Im}\lambda_t$ ,  $\text{Re}\lambda_t$ ,  $\varepsilon'/\varepsilon$  and branching

Quantity	Central	Error
$ V_{cb} $	0.040	$\pm 0.002$
$ V_{ub} $	$3.56 \cdot 10^{-3}$	$\pm 0.56 \cdot 10^{-3}$
$m_c$	1.3 GeV	0.1 GeV
$m_t$	165 GeV	$\pm 5$ GeV
$\hat{B}_K$	0.80	$\pm 0.15$
$\sqrt{B_d} F_{B_d}$	200 MeV	$\pm 40$ MeV
$(\Delta M)_d$	$0.471 \text{ ps}^{-1}$	$\pm 0.016 \text{ ps}^{-1}$
$(\Delta M)_s$	$> 14.6 \text{ ps}^{-1}$	95% C.L.
$\xi$	1.16	$\pm 0.07$
$\Lambda_{\overline{\text{MS}}}^{(4)}$	340 MeV	$\pm 50$ MeV
$m_s(m_c)$	130 MeV	$\pm 25$ MeV
$B_6^{(1/2)}$	1.0	$\pm 0.3$
$B_8^{(3/2)}$	0.8	$\pm 0.2$

Table 3: Collection of SM input parameters.

ratios for rare decays will be generally different in these two models due to new supersymmetric contributions in the one-loop diagrams as summarized in sections 3 and 4. We follow here the strategy B of section 5 as the universal unitarity triangle is unknown at present.

The values of the parameters in table 3 are precisely the ones used in [5] except for the lower bound on  $(\Delta M)_s$  which has been improved since then [86]. The relevant references to table 3 can be found in [5].

The only controversial values in table 3 are the ones for  $B_6^{(1/2)}$ ,  $B_8^{(3/2)}$  and  $m_s$ . Other authors would possibly use different values for these parameters. As one of the main purposes of the present paper is to investigate the impact of supersymmetric contributions on our  $\varepsilon'/\varepsilon$  analysis within the SM [5], we will keep the values of all the SM input parameters as in [5]. Reviews of the values of  $B_6^{(1/2)}$ ,  $B_8^{(3/2)}$  and  $m_s$  used by other authors can be found in [5, 15]. We will briefly comment at the end of this section how our analysis would change had we used different values for  $B_6^{(1/2)}$  and  $B_8^{(3/2)}$ .

## 7.2 Supersymmetric Parameters

As discussed in section 2.2, we will choose the following supersymmetric input parameters:

$$\tilde{m}_{t_1}, \quad \tilde{m}_{t_2}, \quad \theta_{\tilde{t}}, \quad \tilde{m}_{\chi_1}, \quad \tan \beta, \quad m_{H^\pm}, \quad \mu, \quad m_{\tilde{\ell}}, \quad (7.4)$$

where  $\tilde{m}_{t_1}$  and  $\tilde{m}_{t_2}$  are the heavy and light stop mass respectively,  $\theta_{\tilde{t}}$  is the mixing angle in the stop mass matrix,  $\tilde{m}_{\chi_1}$  the light chargino mass,  $\tan\beta$  the ratio of the two Higgs vacuum expectation values,  $m_{H^\pm}$  the charged Higgs mass,  $\mu$  the Higgs superfield mixing parameter and  $m_{\tilde{\ell}}$  is the common slepton mass entering the expressions for rare K and B decays. We now discuss the ranges in which we randomly generate with flat distributions the parameters in eq. (7.4).

The region of SUSY parameter space in which we expect SUSY contributions to  $\varepsilon'/\varepsilon$  to be maximal (in absolute value) corresponds to the case of a light stop and chargino. We therefore allow for the lighter stop and chargino to be as light as allowed by present constraints,

$$90 \text{ GeV} < \tilde{m}_{\chi_1} < 250 \text{ GeV}, \quad 90 \text{ GeV} < \tilde{m}_{t_2} < 800 \text{ GeV}. \quad (7.5)$$

Concerning the stop mixing angle, we generate it in the range  $-\pi/2 < \theta_{\tilde{t}} < \pi/2$ . The case of a very light and right-handed  $\tilde{t}_2$  requires  $\tilde{m}_{\tilde{t}_R}^2 < 0$ . This might however induce charge and colour breaking minima in the potential. To avoid this, following ref. [87] we impose the bound

$$\tilde{m}_{\tilde{t}_R}^2 > - \left( \frac{M_h^2(v_1^2 + v_2^2)g_s}{12} \right)^{\frac{1}{2}}, \quad (7.6)$$

which for a typical Higgs mass  $M_h \sim 90 \text{ GeV}$  amounts to  $\tilde{m}_{\tilde{t}_R}^2 \gtrsim -(90 \text{ GeV})^2$ . We also impose  $\tilde{m} > 250$ : Since minimal flavour violation requires the soft breaking left-handed squark mass to be universal, this implies  $\tilde{m}_{t_2} \gtrsim 300 \text{ GeV}$  for  $\theta_{\tilde{t}} \sim \pm\pi/2$ .

We vary the charged Higgs mass in the range  $100 \text{ GeV} < m_{H^\pm} < 1 \text{ TeV}$ , and choose  $|\mu| < 500 \text{ GeV}$ . In this work, we do not analyze possible effects in the large  $\tan\beta$  regime, where additional operators can arise. We can therefore limit ourselves to the region  $1.2 < \tan\beta < 6$ , since the dependence on  $\tan\beta$  becomes very weak already for  $\tan\beta > 3$ , until one enters the large  $\tan\beta$  regime. Finally, we impose  $\tilde{m}_{t_1} < 1 \text{ TeV}$  and  $90 \text{ GeV} < \tilde{m}_{\ell} < 500 \text{ GeV}$ . We do not enforce GUT relations between SUSY parameters since we are considering a more general class of theories described in terms of the SUSY parameters at the electroweak scale, with no reference to the structure of the theory at higher scales. The NLO calculation adopted for  $BR(b \rightarrow s\gamma)$  introduces a dependence also on the gluino mass  $\tilde{m}_g$ , which we choose to vary in the range  $250 \text{ GeV} < \tilde{m}_g < 1 \text{ TeV}$ .

We scan the parameter space specified above and impose the constraints discussed in section 6. Then for the points allowed by these constraints we perform the determination of  $\text{Im}\lambda_t$  and  $\text{Re}\lambda_t$  from  $\Delta F = 2$  processes and then compute  $\varepsilon'/\varepsilon$  and branching ratios for rare decays. We provide the details of this computation below.

The ranges for supersymmetric input parameters are summarized in table 4.



Quantity	Min	Max
$\tilde{m}_{t_1}$	90 GeV	1 TeV
$\tilde{m}_{t_2}$	90 GeV	800 GeV
$\theta_{\tilde{t}}$	$-\pi/2$	$\pi/2$
$\tilde{m}_{\chi_1}$	90 GeV	250 GeV
$\tilde{m}_g$	250 GeV	1 TeV
$\tan \beta$	1.2	6
$m_{H^\pm}$	100 GeV	1 TeV
$\mu$	-500 GeV	500 GeV
$\tilde{m}_\ell$	90 GeV	500 GeV

Table 4: Collection of supersymmetric input parameters.

### 7.3 Strategy

The uncertainties in the input parameters of table 3 screen considerably the effects of supersymmetric contributions. In order to study various trends and patterns of supersymmetric effects in  $\text{Im}\lambda_t$ ,  $\text{Re}\lambda_t$ ,  $\varepsilon'/\varepsilon$  and rare decays we proceed as follows:

**Step 1:**

We set the SM parameters to their central values in table 3 and, using a random generation of  $\sim 6 \cdot 10^6$  points, calculate the ranges for the ratios

$$K(F_r) = \frac{(F_r)_{\text{MSSM}}}{(F_r)_{\text{SM}}}, \quad F_r = X, Y, Z, E, S, X^{(\nu\bar{\nu})}, Y^{(e\bar{e})} \quad (7.7)$$

with  $(F_r)_{\text{SM}}$  and  $(F_r)_{\text{MSSM}}$  representing the SM and total contributions to the functions in question respectively.  $S \equiv F_{tt}$  with  $F_{tt}$  given in (4.5). These ratios are of interest for both strategies of section 5. In order to investigate the impact of various constraints on SUSY parameters we consider the following cases:

1. Only the constraints from  $\varepsilon$ ,  $B_{d,s}^0 - \bar{B}_{d,s}^0$ - mixings and direct bounds on masses of squarks, sleptons, charginos and charged Higgs particles are imposed.
2. The additional constraint from  $B \rightarrow X_s \gamma$  is imposed.
3. The additional constraint from  $\Delta\varrho$  is imposed without any constraint from  $B \rightarrow X_s \gamma$ .
4. The additional constraint from the lower bound on the neutral Higgs mass is imposed without any constraint from  $B \rightarrow X_s \gamma$  and  $\Delta\varrho$ .

5. All constraints are taken into account.

This step allows us to identify the dominant supersymmetric contributions.

**Step 2:**

We repeat the analysis of Step 1 calculating this time the ranges for the ratios

$$T(\varepsilon'/\varepsilon) = \frac{(\varepsilon'/\varepsilon)_{\text{MSSM}}}{(\varepsilon'/\varepsilon)_{\text{SM}}} \quad (7.8)$$

and analogous ratios for  $\text{Im}\lambda_t$ ,  $\text{Re}\lambda_t$ , and the branching ratios for rare decays.

We also investigate for which sets of supersymmetric parameters the maximal and minimal values of these ratios are obtained.

**Step 3:**

We repeat the analysis of Step 2 in the case of  $\varepsilon'/\varepsilon$ , investigating the dependence of  $T(\varepsilon'/\varepsilon)$  on  $B_6^{(1/2)}$ .

## 7.4 Results of Step 1

Our analysis shows that, taking only the constraints (1) into account, supersymmetric contributions to the box functions  $B^{(u)}$ ,  $B^{(d)}$  and  $B^{(\nu\bar{\nu})}$  amount respectively to at most 4%, 7% and 11% of their SM values and are suppressed below 3%, 6% and 11% after all constraints are taken into account. These effects are only relevant in the case of the function  $X$  where the box function enters with an additional factor 4. The supersymmetric contributions to the functions  $|B^{(e\bar{e})}|$ ,  $C$ ,  $|D|$ ,  $E$  and  $S$  can be as high as +34%, +51%, +93%, +107% and +159% respectively if no constraints from  $B \rightarrow X_s\gamma$ ,  $\Delta\varrho$  and  $(M_h)_{\min}$  are imposed. While  $S$  is always enhanced,  $C$ ,  $|D|$  and  $E$  can be suppressed up to 24%, 7% and 17% respectively. The constraints (2–5) turn out to have only a minor impact on the functions  $B^{(e\bar{e})}$ ,  $D$ ,  $E$  and  $S$ . On the other hand the maximal enhancement of  $C$  is reduced to 29%.

The function  $E$  is absent in  $K^+ \rightarrow \pi^+\nu\bar{\nu}$ ,  $K_L \rightarrow \pi^0\nu\bar{\nu}$ ,  $B \rightarrow X_s\nu\bar{\nu}$  and  $B_s \rightarrow \mu\bar{\mu}$ , and plays only a minor role in  $\varepsilon'/\varepsilon$  and a negligible role in  $K_L \rightarrow \pi^0 e^+ e^-$ . Consequently its modification is immaterial for our analysis. On the other hand the enhancement of  $S$  can have considerable impact on the values of  $\text{Im}\lambda_t$  and  $\text{Re}\lambda_t$  as we will see below. Similarly the supersymmetric effects in the functions  $C$  and  $D$  are sizable, although these effects are less visible in the functions  $X$ ,  $Y$ ,  $Z$  due to various cancellations between box and penguin contributions.

In table 5 we show the minimal and maximal values of the ratios  $K(F_r)$  defined in (7.7) in the case of no constraints from  $B \rightarrow X_s\gamma$ ,  $\Delta\varrho$  and  $(M_h)_{\min}$  and after the imposition of these constraints. The anatomy of these three constraints is shown in table 6. In the case

	No Constraints		All Constraints	
$K(F_r)$	<b>min</b>	<b>max</b>	<b>min</b>	<b>max</b>
$K(B^{(u)})$	0.96	1.00	0.97	1.00
$K(B^{(d)})$	0.93	1.01	0.94	1.01
$K(B^{(\nu\bar{\nu})})$	0.89	1.01	0.89	1.01
$K(B^{(e\bar{e})})$	0.94	1.34	0.96	1.34
$K(C)$	0.76	1.51	0.76	1.29
$K(D)$	0.93	1.93	0.95	1.87
$K(X)$	0.87	1.26	0.87	1.15
$K(Y)$	0.81	1.41	0.81	1.23
$K(Z)$	0.68	1.65	0.70	1.35
$K(E)$	0.83	2.07	0.83	1.85
$K(S)$	1.01	2.59	1.01	2.13
$K(X^{(\nu\bar{\nu})})$	0.83	1.25	0.85	1.15
$K(Y^{(e\bar{e})})$	0.82	1.41	0.82	1.24
$K(F_{\epsilon'})$	0.59	1.27	0.76	1.23

Table 5: The minimal and maximal values of the the ratios  $K(F_r)$  without constraints and with all constraints taken into account.

of the functions  $E$  and  $S$  we observe the features just discussed. The supersymmetric effects in the functions  $X$ ,  $Y$  and  $Z$  can be at most  $\pm 15\%$ ,  $\pm 23\%$  and  $\pm 35\%$  respectively after all constraints have been imposed. This is related to the fact that while the function  $C$  is positive, the function  $D$  is negative. Consequently the observed enhancement of  $|D|$  results in a suppression of  $Z$ . This suppression is reduced by the factor  $1/4$  with which the function  $D$  enters the function  $Z$  and by the enhancement of  $C$ , which for certain values of supersymmetric parameters can overcompensate the suppression of  $Z$  through  $D$  so that an enhancement of  $Z$  is possible.

It should be stressed that in the two Higgs doublet model the function  $Z$  is always enhanced through charged Higgs effects. The possible suppression of  $Z$  in the MSSM comes then from chargino exchanges that are particularly important in the photon penguin function  $D$ .

Let us now identify the region of SUSY parameter space where the maximal deviations from the SM are possible. The function  $S$  takes its largest values for a light, mainly right-handed stop, with a large splitting between the stops, and small  $\tan\beta$  (see fig. 2). The function  $C$  reaches its maximal values for small  $\tan\beta$  and large stop mixing, while the

	$B \rightarrow X_s \gamma$ only		$\Delta \varrho$ only		$(M_h)_{min}$ only	
$K(F_r)$	min	max	min	max	min	max
$K(B^{(u)})$	0.96	1.00	0.96	1.00	0.96	1.00
$K(B^{(d)})$	0.93	1.01	0.94	1.01	0.93	1.01
$K(B^{(\nu\bar{\nu})})$	0.89	1.01	0.89	1.01	0.89	1.01
$K(B^{(e\bar{e})})$	0.95	1.34	0.94	1.34	0.95	1.34
$K(C)$	0.76	1.51	0.76	1.39	0.76	1.51
$K(D)$	0.93	1.93	0.93	1.93	0.94	1.87
$K(X)$	0.87	1.26	0.87	1.20	0.87	1.26
$K(Y)$	0.81	1.41	0.81	1.31	0.81	1.41
$K(Z)$	0.68	1.65	0.68	1.47	0.70	1.65
$K(E)$	0.83	2.07	0.83	2.07	0.83	1.85
$K(S)$	1.01	2.59	1.01	2.59	1.01	2.18
$K(X^{(\nu\bar{\nu})})$	0.83	1.25	0.83	1.20	0.85	1.25
$K(Y^{(e\bar{e})})$	0.82	1.41	0.82	1.31	0.82	1.41
$K(F_{\epsilon'})$	0.61	1.27	0.68	1.27	0.59	1.23

Table 6: The anatomy of various constraints on the minimal and maximal values of the ratios  $K(F_r)$ .

minimal values are attained for a light, mainly right-handed stop and light chargino (see fig. 3). The function  $|D|$  is almost always larger than in the SM, and reaches its maximum for a light, mainly right-handed stop, a light chargino and small  $\mu$  (see fig. 4). Therefore,  $Z$  is enhanced with respect to the SM for small  $\tan \beta$  and large stop mixing, and suppressed for a light, mainly right-handed stop and light chargino (See fig. 5).

As seen in table 6 the constraints from  $\Delta \varrho$  and the lower bound on  $H^0$  mass are slightly more effective than the constraint from  $B \rightarrow X_s \gamma$ . Yet the comparison of tables 5 and 6 shows that the inclusion of all bounds simultaneously eliminates a range of possible values for  $X$ ,  $Y$  and  $Z$  which are allowed if each constraint is imposed separately.

To evaluate the effect of the bounds discussed in section 6, we show in fig. 6 the ranges for  $K(S)$  and  $K(C)$  without applying the constraints: the comparison with figs. 2 and 3 clearly shows the impact of the bounds.

From the above considerations it is clear that any future increase in the lower bounds on  $M_h$  and  $\tan \beta$  will considerably reduce the possible enhancements of  $S$  and  $Z$ , and therefore, as we shall see in the following, the possible suppression of  $\varepsilon'/\varepsilon$ .

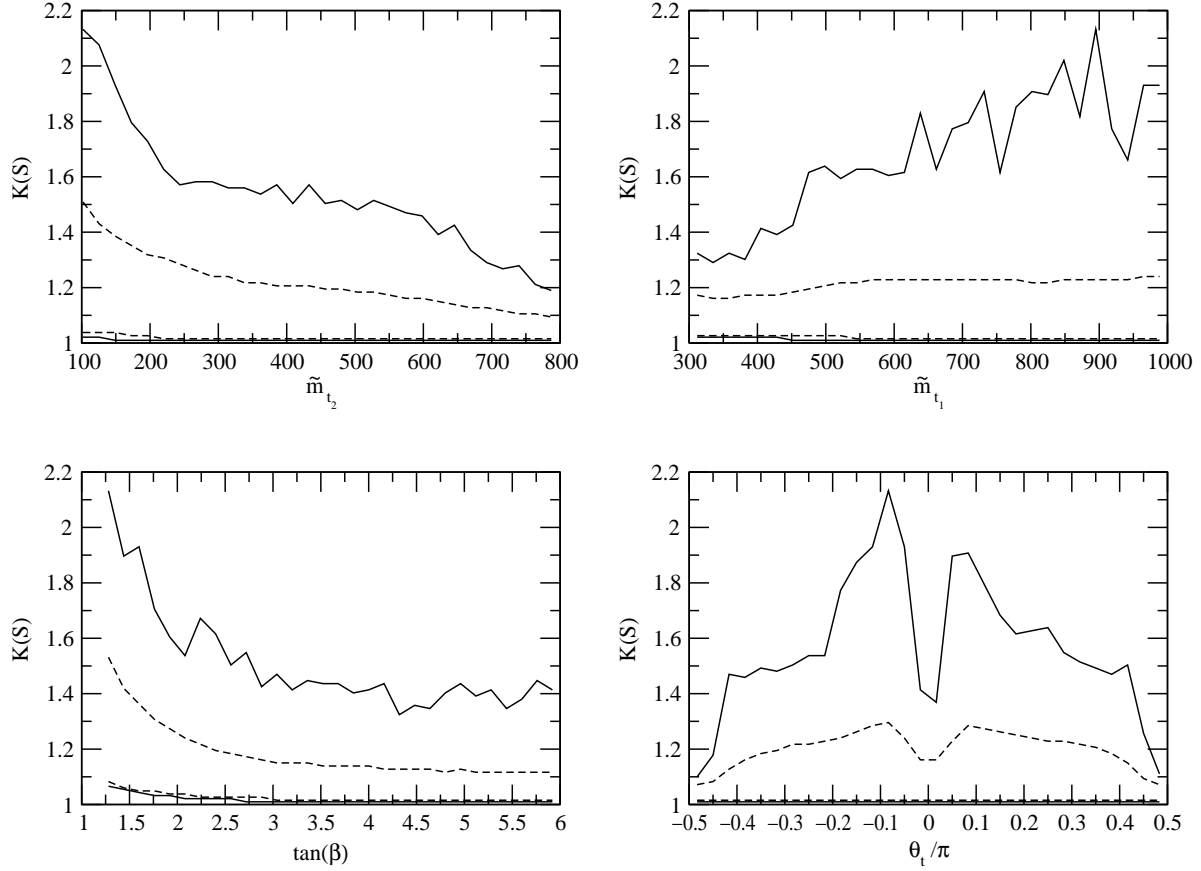


Figure 2: Contour plots of  $K(S)$  as a function of  $\tilde{m}_{t_2}$ ,  $\tilde{m}_{t_1}$ ,  $\tan\beta$  and  $\theta_{\tilde{t}}$ , including all the constraints discussed in section 6. The dashed and continuous lines contain 95% and 100% of the allowed points respectively.

## 7.5 Results of Step 2

In table 7 we show the minimal and maximal values of the ratios  $T$  defined in (7.8) in the case of no constraints from  $B \rightarrow X_s \gamma$ ,  $\Delta\varrho$  and  $(M_h)_{min}$  and after the imposition of these bounds. The anatomy of these three constraints is shown in table 8. We make the following observations, taking all the constraints into account:

- The extracted  $\text{Im}\lambda_t$  and  $|\text{Re}\lambda_t|$  are suppressed by supersymmetric contributions. This is related to the enhancement of  $F_{tt}$  in the MSSM.
- $\varepsilon'/\varepsilon$  can be enhanced by at most 7% but can be suppressed even by a factor of 2. This pattern agrees with the one found in [37] although the supersymmetric effects in  $\varepsilon'/\varepsilon$  found here are smaller than in [37] due to the tighter constraints on supersymmetric parameters imposed in the present analysis. We will elaborate on

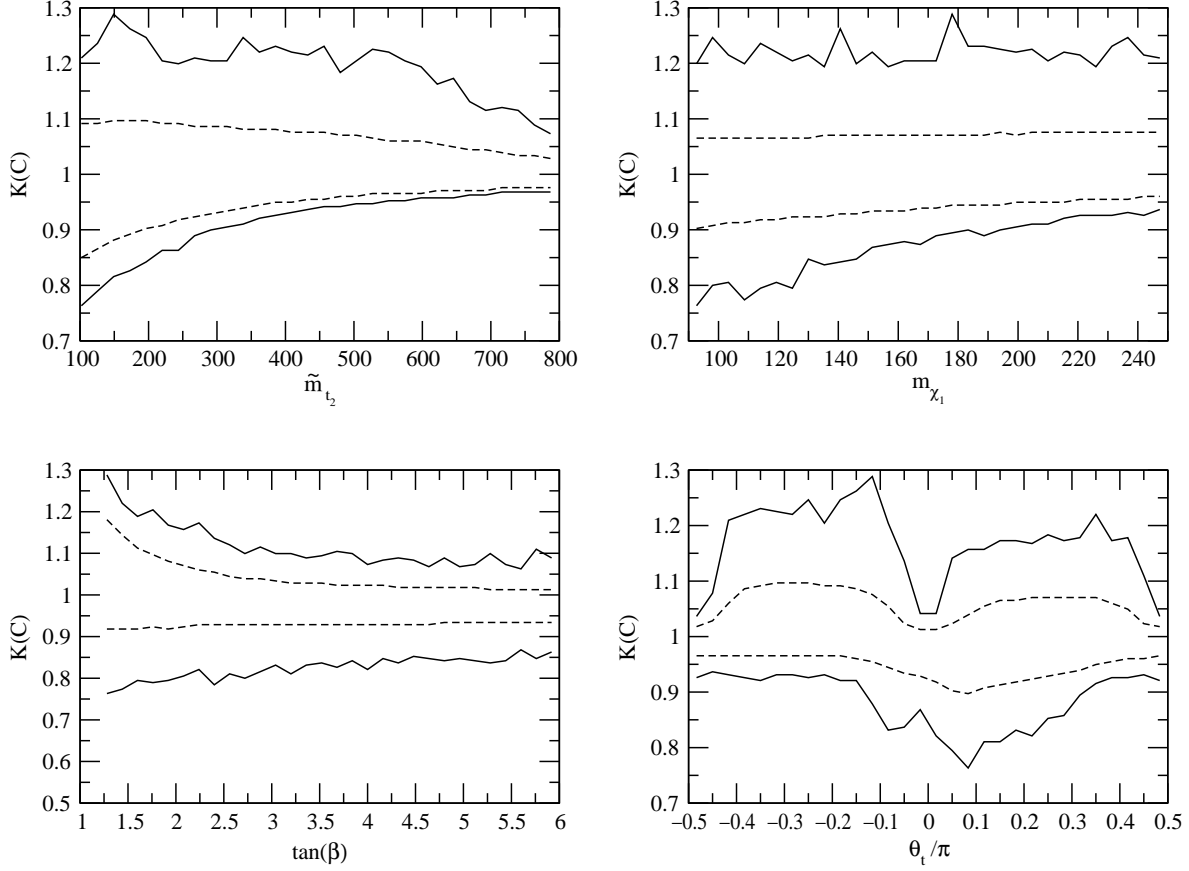


Figure 3: Contour plots of  $K(C)$  as a function of  $\tilde{m}_{t_2}$ ,  $\tilde{m}_{t_1}$ ,  $\tan\beta$  and  $\theta_{\tilde{t}}$ , including all the constraints discussed in section 6. The dashed and continuous lines contain 95% and 100% of the allowed points respectively.

these results below.

- The branching ratios for  $K^+ \rightarrow \pi^+ \nu \bar{\nu}$ ,  $K_L \rightarrow \pi^0 \nu \bar{\nu}$  and  $K_L \rightarrow \pi^0 e^+ e^-$  are basically suppressed by supersymmetric contributions relative to the SM expectations. The suppression of  $Br(K^+ \rightarrow \pi^+ \nu \bar{\nu})$  can be at most 35%. The corresponding suppressions in  $K_L \rightarrow \pi^0 \nu \bar{\nu}$  and  $K_L \rightarrow \pi^0 e^+ e^-$  can be as high as a factor of 2.5 and 2 respectively. As seen in (5.12), (5.13) and (5.15) and tables 5 and 7, these suppressions are related to the suppressions of  $\text{Im}\lambda_t$  and  $|\text{Re}\lambda_t|$  that cannot be compensated by possible enhancements of the functions  $X$ ,  $Y$  and  $Z$ .
- As expected on the basis of (5.16) and (5.17) the pattern of supersymmetric effects is different for the rare decays  $B \rightarrow X_s \nu \bar{\nu}$  and  $B_s \rightarrow \mu \bar{\mu}$ . Here possible enhancements and suppressions can be directly calculated using (5.16), (5.17) and table 5. The supersymmetric effects in  $Br(B \rightarrow X_s \nu \bar{\nu})$  can be at most  $\pm 34\%$ .  $Br(B_s \rightarrow \mu \bar{\mu})$  can

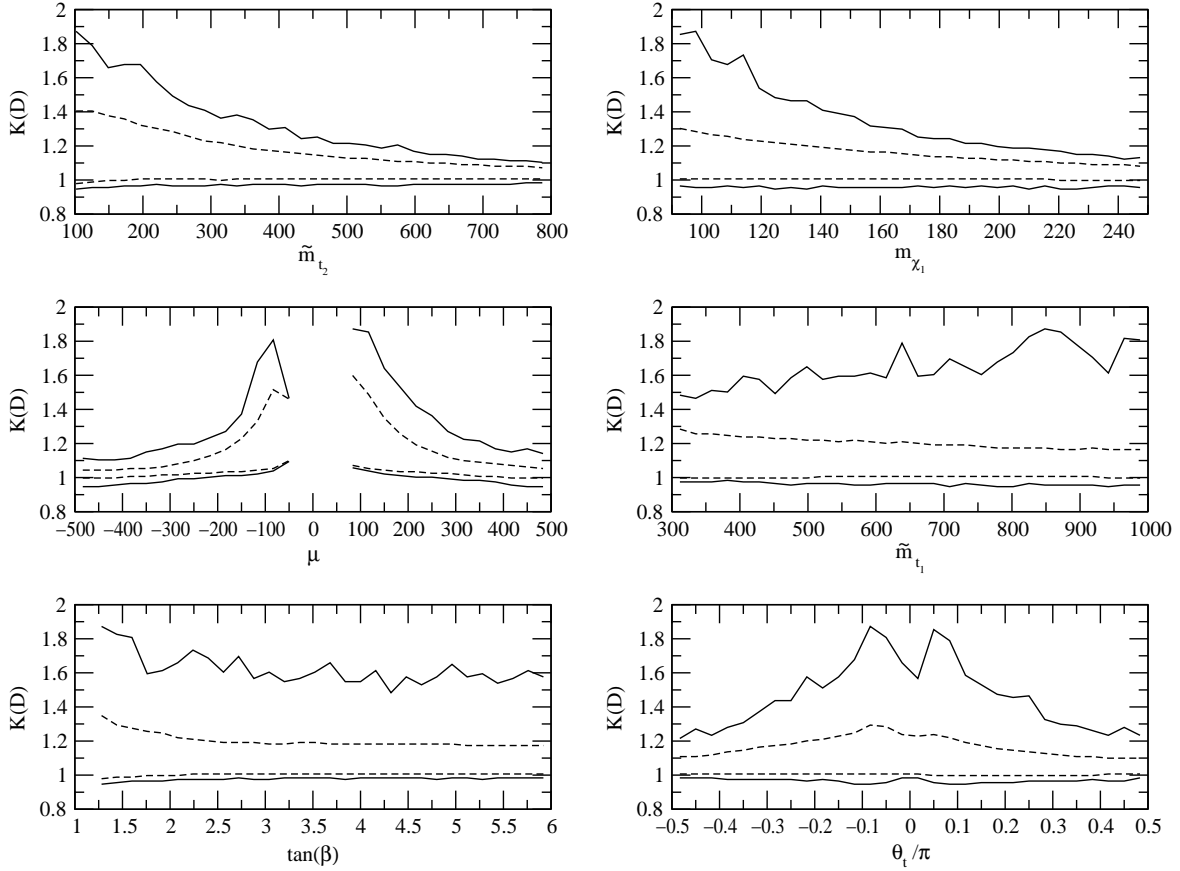


Figure 4: Contour plots of  $K(D)$  as a function of  $\tilde{m}_{t_2}$ ,  $\tilde{m}_{\chi_1}$ ,  $\mu$ ,  $\tilde{m}_{t_1}$ ,  $\tan\beta$  and  $\theta_{\tilde{t}}$ , including all the constraints discussed in section 6. The dashed and continuous lines contain 95% and 100% of the allowed points respectively.

be enhanced up to 53% and suppressed up to 32%.

## 7.6 General Patterns: $\varepsilon'/\varepsilon$

Let us elaborate on our results for  $\varepsilon'/\varepsilon$ . The dominant supersymmetric contributions to  $\varepsilon$  and  $(\Delta M)_{d,s}$  originate in the functions  $S_H(t, t)$  and  $S_\chi(t, t)$  contributing to  $F_{tt}$  in (4.5). These two functions add positive contributions to  $F_{tt}$  which is positive in the SM. As a result, the values of  $\text{Im}\lambda_t$  and  $|\text{Re}\lambda_t|$  in the MSSM are smaller than in the SM for any choice of the supersymmetric parameters in (7.4). This is clearly seen in table 7. The suppressions of  $\text{Im}\lambda_t$  and  $|\text{Re}\lambda_t|$  are largest for a very light, mainly right-handed stop, for a large splitting between the stops, for small  $\tilde{m}_{\chi_1}$  and small  $\tan\beta$ .

The dominant supersymmetric contributions to  $F_{\varepsilon'}$  in (4.10) originate in supersymmetric contributions to the function  $Z$  in (4.11) which results from  $Z^0$ -penguin diagrams

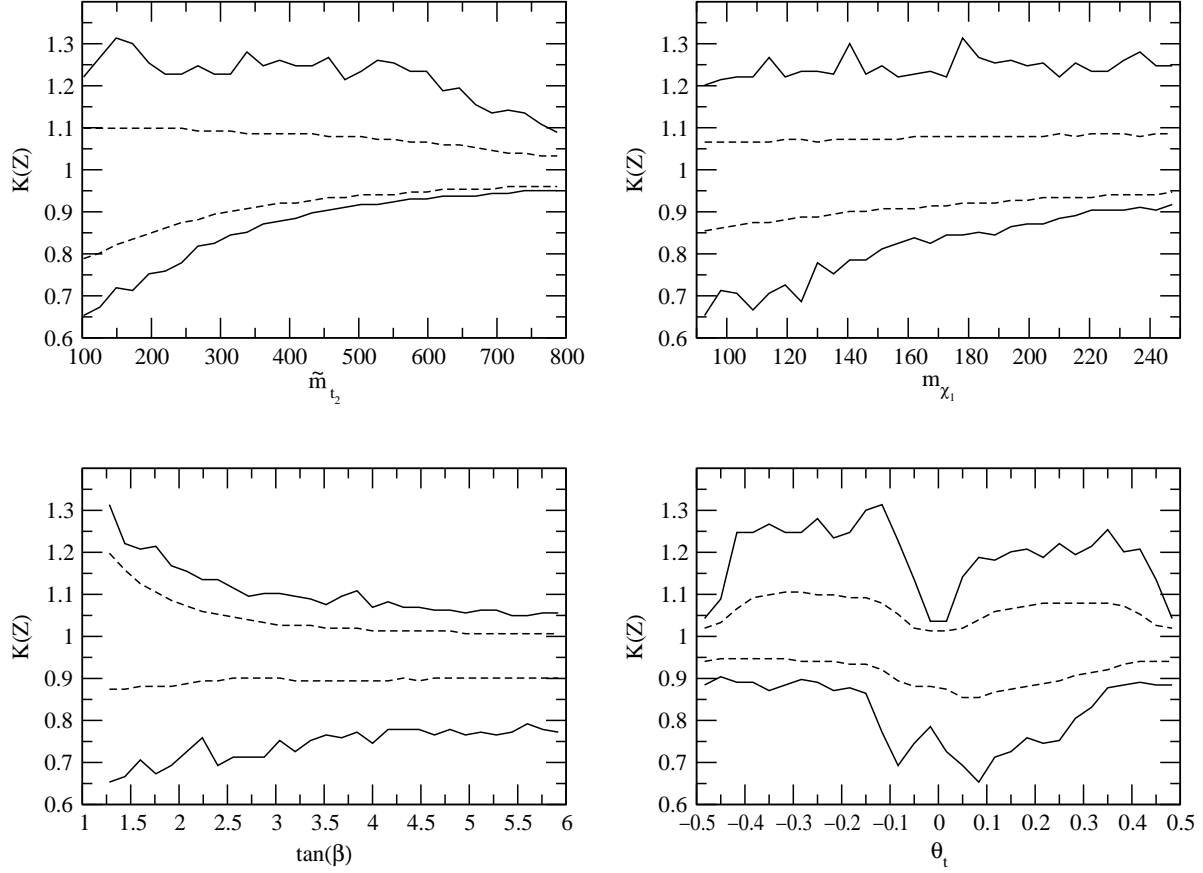


Figure 5: Contour plots of  $K(Z)$  as a function of  $\tilde{m}_{t_2}$ ,  $\tilde{m}_{t_1}$ ,  $\tan\beta$  and  $\theta_{\tilde{t}}$ , including all the constraints discussed in section 6. The dashed and continuous lines contain 95% and 100% of the allowed points respectively.

and photon-penguin diagrams. The corresponding contributions to the functions  $X$ ,  $Y$ , and  $E$  have a considerably smaller impact on  $F_{\varepsilon'}$ . This is related to a large extent to the fact that the coefficient  $P_Z$  in (4.10) is substantially larger than the coefficients  $P_X$ ,  $P_Y$  and  $P_E$ .

Setting the parameters of tables 2 and 3 to their central values we find

$$F_{\varepsilon'} = 10.3 - 7.7 \cdot Z + 1.1 \quad (7.9)$$

where the last term represents the contributions of  $X$ ,  $Y$  and  $E$  evaluated within the SM. The first term represents the part unaffected by supersymmetric contributions. It is dominated by the contribution of the QCD-penguin operators, whose Wilson coefficients are strongly enhanced by renormalization group evolution from scales  $\mathcal{O}(M_W)$  to scales  $\mathcal{O}(1 \text{ GeV})$ . As stated above, the supersymmetric contributions affect  $F_{\varepsilon'}$  dominantly through the function  $Z$ , which equals 0.66 in the SM.



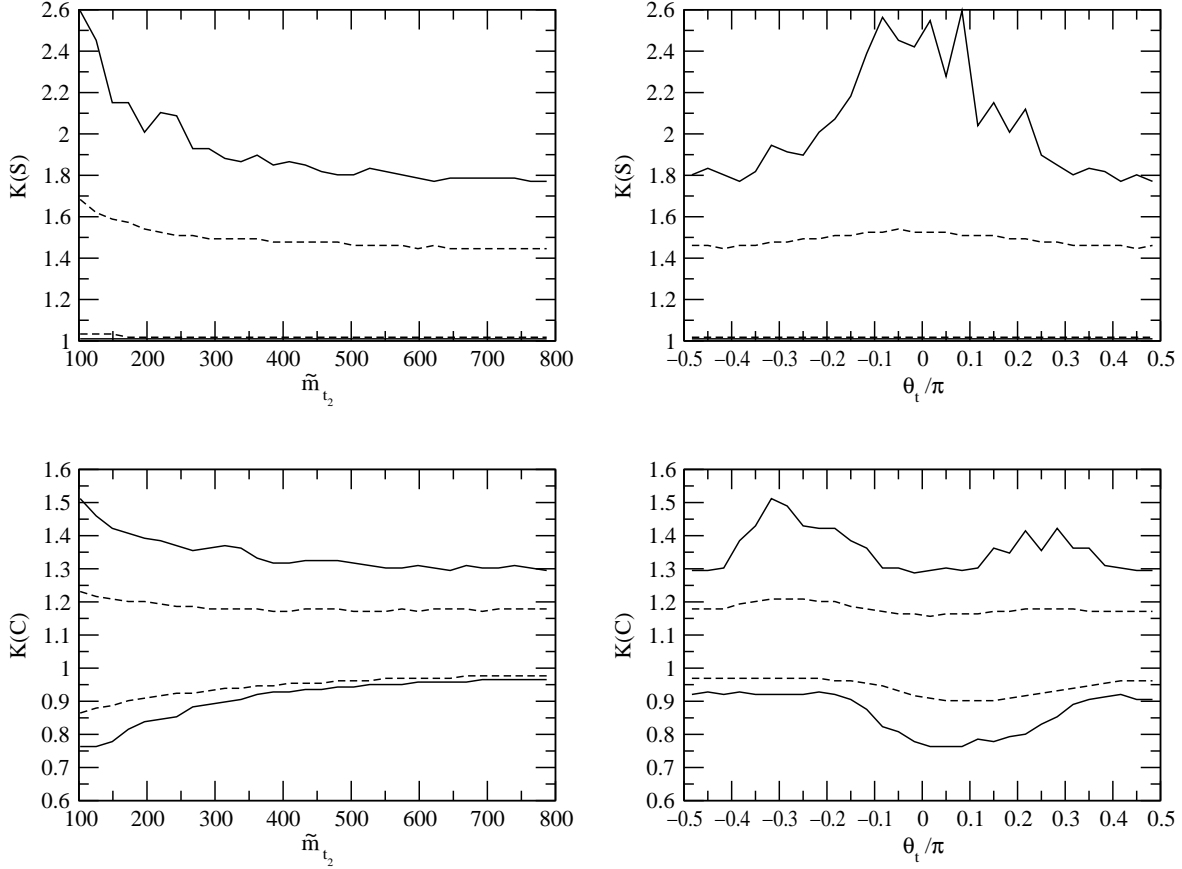


Figure 6: Contour plots of  $K(S)$  and  $K(C)$  as a function of  $\tilde{m}_{t_2}$  and  $\theta_{\tilde{t}}$ , without imposing the constraints discussed in section 6. The dashed and continuous lines contain 95% and 100% of the generated points respectively.

The charged Higgs contribution to the function  $Z$  is positive for any value of  $\tan\beta$  and  $m_{H^\pm}$ . Consequently, as seen in (7.9), this contribution suppresses  $F_{\varepsilon'}$  and  $\varepsilon'/\varepsilon$ . This suppression of  $\varepsilon'/\varepsilon$  is enhanced by the suppression of  $\text{Im}\lambda_t$  through charged Higgs contributions as discussed above. A detailed numerical analysis of these effects within the two Higgs doublet model has been presented in [5, 52]

As pointed out in [37], depending on the choice of the supersymmetric parameters, the chargino contribution to the function  $Z$  and more generally to  $F_{\varepsilon'}$  can have either sign. Indeed as seen in table 5 the function  $Z$  can be suppressed up to 30% relative to its SM value even if all constraints are imposed. If this happens the suppression of  $\varepsilon'/\varepsilon$  due to  $Z^0$ -penguins observed in the SM and in the two-Higgs doublet model becomes smaller.

Whether  $\varepsilon'/\varepsilon$  can be enhanced in MSSM over the SM prediction depends on whether the positive contribution of charginos to the function  $F_{\varepsilon'}$  can overcompensate the corresponding negative charged Higgs contribution to this function and the suppression of  $\text{Im}\lambda_t$

	No Constraints		All Constraints	
$T$	<b>min</b>	<b>max</b>	<b>min</b>	<b>max</b>
$T(\text{Im}\lambda_t)$	0.57	1.00	0.66	1.00
$T(\text{Re}\lambda_t)$	0.78	1.00	0.81	1.00
$T(\varepsilon'/\varepsilon)$	0.42	1.07	0.53	1.07
$T(K^+ \rightarrow \pi^+ \nu \bar{\nu})$	0.59	1.09	0.65	1.02
$T(K_L \rightarrow \pi^0 \nu \bar{\nu})$	0.28	1.12	0.41	1.03
$T(K_L \rightarrow \pi^0 e^+ e^-)$	0.33	1.10	0.48	1.10
$T(B \rightarrow X_s \nu \bar{\nu})$	0.70	1.60	0.73	1.34
$T(B_s \rightarrow \mu \bar{\mu})$	0.68	1.99	0.68	1.53

Table 7: The minimal and maximal values of the the ratios  $T$  without constraints and with all constraints taken into account.

	$B \rightarrow X_s \gamma$ only		$\Delta \varrho$ only		$(M_h)_{min}$ only	
$T$	<b>min</b>	<b>max</b>	<b>min</b>	<b>max</b>	<b>min</b>	<b>max</b>
$T(\text{Im}\lambda_t)$	0.57	1.00	0.57	1.00	0.64	1.00
$T(\text{Re}\lambda_t)$	0.78	1.00	0.78	1.00	0.80	1.00
$T(\varepsilon'/\varepsilon)$	0.42	1.07	0.46	1.07	0.42	1.07
$T(K^+ \rightarrow \pi^+ \nu \bar{\nu})$	0.59	1.08	0.59	1.02	0.65	1.09
$T(K_L \rightarrow \pi^0 \nu \bar{\nu})$	0.28	1.12	0.28	1.03	0.41	1.12
$T(K_L \rightarrow \pi^0 e^+ e^-)$	0.33	1.10	0.33	1.10	0.48	1.10
$T(B \rightarrow X_s \nu \bar{\nu})$	0.70	1.60	0.70	1.46	0.73	1.60
$T(B_s \rightarrow \mu \bar{\mu})$	0.68	1.99	0.68	1.73	0.68	1.99

Table 8: The anatomy of various constraints on the minimal and maximal values of the the ratios  $T$ .

due to supersymmetric contributions. While the chargino contribution to  $F_{\varepsilon'}$  can indeed overcompensate the corresponding negative charged Higgs contribution (see Table 5) the resulting enhancement of  $F_{\varepsilon'}$  is generally insufficient to cancel the suppression of  $\text{Im}\lambda_t$ . Consequently for the dominant part of the allowed values of supersymmetric parameters  $\varepsilon'/\varepsilon$  in MSSM is suppressed with respect to its SM estimate. This is clearly seen in the contour plots in fig. 7 where we show the range for  $\varepsilon'/\varepsilon$  as a function of  $\tilde{m}_{t_2}$ ,  $\tilde{m}_{t_1}$ ,  $\tan\beta$  and  $\theta_{\tilde{t}}$ , with other parameters varied in the allowed ranges. The strongest suppression of  $\varepsilon'/\varepsilon$  takes place for lowest  $\tan\beta$ ,  $m_{H^\pm}$ , for a light, mainly right-handed stop and for large splitting between the stops. The enhancement of  $\varepsilon'/\varepsilon$  over its SM value is found for large

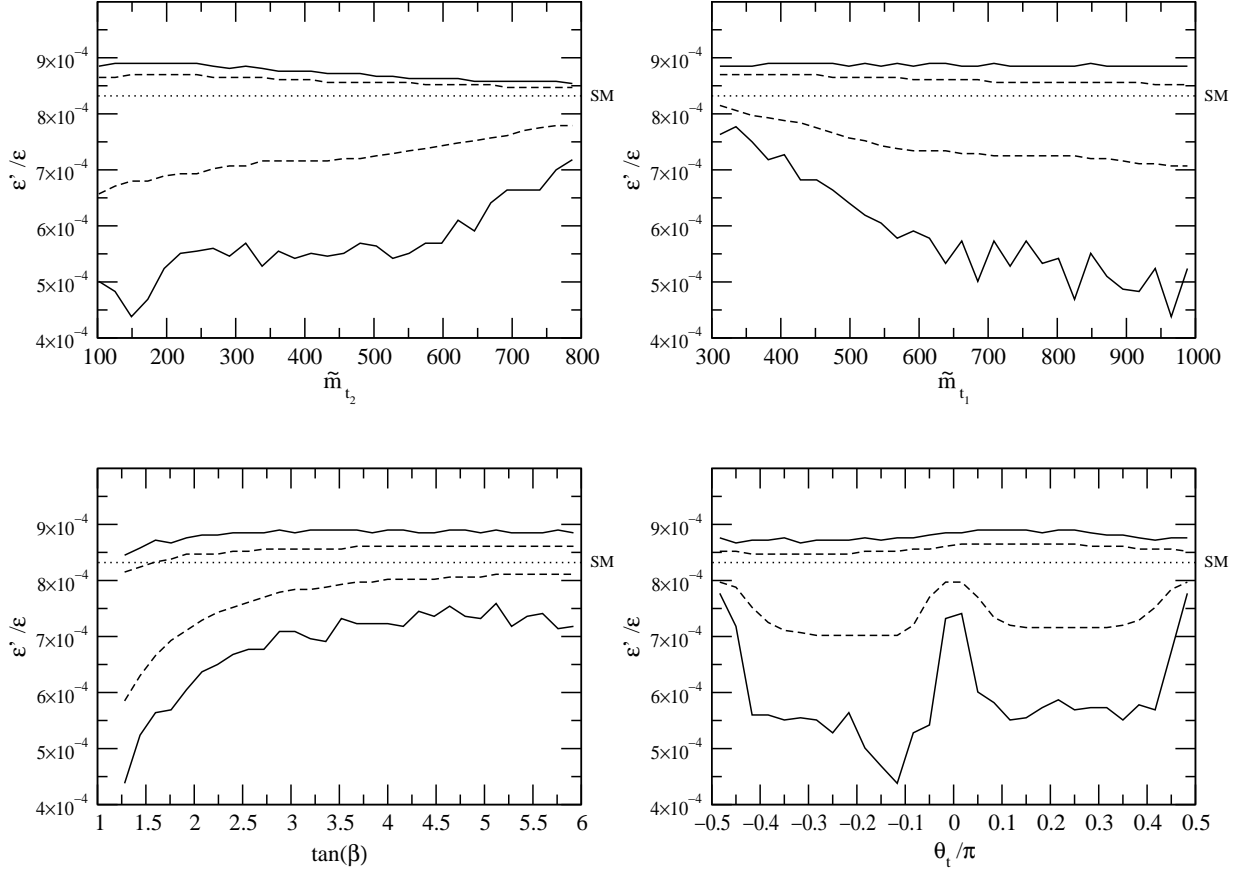


Figure 7: Contour plots of  $\varepsilon'/\varepsilon$  as a function of  $\tilde{m}_{t_2}$ ,  $\tilde{m}_{t_1}$ ,  $\tan\beta$  and  $\theta_{\tilde{t}}$ , imposing the constraints discussed in section 6. The dashed and continuous curves contain 95% and 100% of the allowed points respectively. The dashed horizontal line corresponds to the SM prediction for central values of the parameters in table 3.

$\tan\beta$  and  $m_{H^\pm}$  and small  $m_{\chi_1}$ . In this case the charged Higgs contribution becomes much smaller than the chargino contribution and the enhancement of  $F_{\varepsilon'}$  through the chargino contribution can overcompensate the suppression of  $\text{Im}\lambda_t$ .

Finally, let us comment on the dependence of the above results on the hadronic parameters entering  $\varepsilon'/\varepsilon$ . It is well known that for central values of the parameters in table 3 there is a strong cancellation between QCD and electroweak penguin contributions, as shown explicitly in eq. (7.9). In this case, the enhancement or suppression of electroweak penguins due to SUSY contributions has a relatively large impact on the value of  $\varepsilon'/\varepsilon$ . If, however,  $B_6^{(1/2)}$  is larger than one,  $\varepsilon'/\varepsilon$  becomes more QCD-penguin dominated, the cancellation becomes much less effective and therefore also SUSY contributions have a smaller impact on the value of  $\varepsilon'/\varepsilon$  (as discussed above, the main contribution to QCD penguins

		No Constraints		All Constraints	
$B_6^{(1/2)}$	$T, K$	<b>min</b>	<b>max</b>	<b>min</b>	<b>max</b>
1.0	$K(F_{\varepsilon'})$	0.59	1.27	0.76	1.23
1.0	$T(\varepsilon'/\varepsilon)$	0.42	1.07	0.53	1.07
1.5	$K(F_{\varepsilon'})$	0.78	1.13	0.87	1.11
1.5	$T(\varepsilon'/\varepsilon)$	0.53	1.02	0.60	1.02
2.0	$K(F_{\varepsilon'})$	0.85	1.08	0.91	1.07
2.0	$T(\varepsilon'/\varepsilon)$	0.55	1.00	0.63	1.00

Table 9: The minimal and maximal values of the ratios  $K(F_{\varepsilon'})$  and  $T(\varepsilon'/\varepsilon)$  for different values of  $B_6^{(1/2)}$ , without constraints and with all constraints taken into account.

at the hadronic scale comes from the mixing with current-current operators in the RGE evolution, and is therefore independent of SUSY contributions). This is clearly displayed in table 9, where we report the extremal values of  $K(F_{\varepsilon'})$  and  $T(\varepsilon'/\varepsilon)$  for  $B_6^{(1/2)} = 1, 1.5$  and  $2$ . Similarly, increasing and decreasing the value of  $B_8^{(3/2)}$ , the effects of SUSY contributions to  $\varepsilon'/\varepsilon$  are increased and decreased respectively.

## 7.7 Global Analysis

In principle we could next vary all the SM parameters of tables 2 and 3 in order to obtain the full ranges for  $\varepsilon'/\varepsilon$  and for the branching ratios of rare decays in the MSSM. We do not think such an analysis would be very instructive at present. Roughly speaking the full ranges for the quantities considered in this paper can be obtained by using the SM ranges, given for instance in [24], and rescaling them by the enhancement and suppression factors of table 7.

On the other hand we have updated our 1999 analysis of  $(\varepsilon'/\varepsilon)_{SM}$  [5] by modifying simply  $\Omega_{\eta+\eta'} = 0.25$  to  $\Omega_{\eta+\eta'} = 0.16$  recently obtained in [58]. The result in NDR is given in table 1, to be compared with  $\varepsilon'/\varepsilon = (7.7_{-3.5}^{+6.0})$  of our previous analysis.

## 8 Summary

We have analyzed the CP violating ratio  $\varepsilon'/\varepsilon$  and rare K and B decays in the MSSM with minimal flavour and CP violation. A compendium of phenomenological formulae that should be useful for future analyses is given in section 4. In this version of the MSSM no new operators beyond those present in the SM contribute and all flavour changing transitions are governed by the CKM matrix. In particular there are no new phases beyond

the CKM phase. This implies that the supersymmetric effects enter various quantities of interest exclusively through the one-loop functions.

In spite of this simplification the analysis is complicated by the fact that in addition to a number of poorly constrained supersymmetric parameters one has to deal with hadronic uncertainties. The latter plague in particular  $\varepsilon'/\varepsilon$  and to a lesser extent  $\varepsilon$  and  $B_{d,s}^0 - \bar{B}_{d,s}^0$  mixings. On top of this there are uncertainties in the CKM parameters. Therefore in order to uncover supersymmetric effects we have set the input parameters like  $|V_{ub}|$ ,  $|V_{cb}|$ ,  $\hat{B}_K$ ,  $B_6^{(1/2)}$ ,  $B_8^{(3/2)}$ , that are insensitive to supersymmetric parameters, to their central values. Imposing subsequently constraints on the supersymmetric parameters coming from  $\varepsilon$ ,  $B_{d,s}^0 - \bar{B}_{d,s}^0$  mixings,  $B \rightarrow X_s \gamma$ ,  $\Delta \rho$  in the electroweak precision studies and from the lower bound on the neutral Higgs mass, we have calculated the MSSM predictions for  $\varepsilon'/\varepsilon$  and rare branching ratios normalized to the SM results. Our findings are summarized in table 7 and in the abstract. The calculated quantities in the K-system are generally suppressed by supersymmetric effects, although a 7% enhancement of  $\varepsilon'/\varepsilon$  is still possible. In the case of  $B \rightarrow X_s \nu \bar{\nu}$  and  $B_s \rightarrow \mu \bar{\mu}$  both suppressions and enhancements in the ballpark of 30 – 50% are still possible. We have pointed out that an improved lower bound on the neutral Higgs mass could considerably reduce the allowed ranges.

In view of very large hadronic uncertainties in  $\varepsilon'/\varepsilon$  it will be very difficult to distinguish the MSSM prediction for this ratio from the one in the SM. If future improved calculations of  $B_6^{(1/2)}$  and  $B_8^{(3/2)}$  will demonstrate indisputably that  $(\varepsilon'/\varepsilon)_{SM}$  is below the experimental data our results show that the MSSM will be of little help to remedy this difficulty. On the other hand if it turns out that  $(\varepsilon'/\varepsilon)_{SM}$  is too large then supersymmetric effects in the MSSM could help to obtain the agreement with data.

As rare decays such as  $K^+ \rightarrow \pi^+ \nu \bar{\nu}$ ,  $K_L \rightarrow \pi^0 \nu \bar{\nu}$ ,  $B \rightarrow X_s \nu \bar{\nu}$  and  $B_s \rightarrow \mu \bar{\mu}$  are theoretically very clean, they offer a much better place to look for supersymmetric effects within the MSSM than  $\varepsilon'/\varepsilon$ . The analyses of these decays will be particularly transparent as soon as  $(\Delta M)_d/(\Delta M)_s$  and the CP violating asymmetry in  $B \rightarrow \psi K_S$  will be precisely measured allowing the construction of the universal unitarity triangle [43]. If it turns out that the data for  $K^+ \rightarrow \pi^+ \nu \bar{\nu}$  and  $K_L \rightarrow \pi^0 \nu \bar{\nu}$  are above the SM expectations, it will become clear than more complicated supersymmetric extensions of the SM than the constrained MSSM considered here are required to understand the experimental results. In the case of  $B \rightarrow X_s \nu \bar{\nu}$  and  $B_s \rightarrow \mu \bar{\mu}$  no such clear conclusions will be possible as both enhancements and suppressions of these branching ratios are allowed. On the other hand with precise data the MSSM predictions could in principle be distinguished from the SM ones.

## Acknowledgments

We would like to thank Manuel Drees for very informative discussions, and specially for switching off our PC during the most important run of this work. This work has been supported in part by the German Bundesministerium für Bildung und Forschung under the contracts 06 TM 874 and 05HT9WOA0. L.S. acknowledges the partial support by the M.U.R.S.T.

## Appendix

Here we collect the functions which enter the basic functions of section 3. We use the notation of [37, 52].

$$\begin{aligned}
S(x, y) &= xy \left\{ \left[ \frac{1}{4} + \frac{3}{2} \frac{1}{1-x} - \frac{3}{4} \frac{1}{(1-x)^2} \right] \frac{\log x}{x-y} + (x \leftrightarrow y) - \frac{3}{4} \frac{1}{(1-x)(1-y)} \right\} \\
L_1(x, y, z) &= xy [F(x, y, z) + F(y, z, x) + F(z, x, y)] \\
L_2(x, y, z) &= xy [xF(x, y, z) + yF(y, z, x) + zF(z, x, y)] \\
L_3(x, y, z) &= \frac{1}{xy} L_2(x, y, z) \\
F(x, y, z) &= \frac{x \log x}{(x-1)(x-y)(x-z)}
\end{aligned}$$

**Box( $\Delta$  S=1)**

$$\begin{aligned}
B_{SM}(x) &= -\frac{x}{4(x-1)} + \frac{x}{4(x-1)^2} \log x \\
B_\chi^u(x, y, z) &= -\frac{1}{xy} L_1(x, y, z) \\
B_\chi^d(x, y, z) &= L_3(x, y, z)
\end{aligned}$$

**$\gamma$ -penguin**

$$\begin{aligned}
D_{SM}(x) &= \frac{x^2(25-19x)}{36(x-1)^3} + \frac{(-3x^4+30x^3-54x^2+32x-8)}{18(x-1)^4} \log x \\
D_H(x) &= \frac{x(47x^2-79x+38)}{108(x-1)^3} + \frac{x(-3x^3+6x-4)}{18(x-1)^4} \log x \\
D_\chi(x) &= \frac{(-43x^2+101x-52)}{108(x-1)^3} + \frac{(2x^3-9x+6)}{18(x-1)^4} \log x
\end{aligned}$$

### $Z^0$ -penguin

$$\begin{aligned}
C_{SM}(x) &= \frac{x(x-6)}{8(x-1)} + \frac{x(3x+2)}{8(x-1)^2} \log x \\
C_H(x) &= \frac{x}{8(x-1)} - \frac{x}{8(x-1)^2} \log x \\
C_\chi^{(1)}(x, y) &= \frac{1}{16(y-x)} \left[ \frac{x^2}{x-1} \log x - \frac{y^2}{y-1} \log y \right] \\
C_\chi^{(2)}(x, y) &= \frac{\sqrt{xy}}{8(y-x)} \left[ \frac{x}{x-1} \log x - \frac{y}{y-1} \log y \right]
\end{aligned}$$

### Gluon-penguin

$$\begin{aligned}
E_{SM}(x) &= \frac{x(x^2 + 11x - 18)}{12(x-1)^3} + \frac{(-9x^2 + 16x - 4)}{6(x-1)^4} \log x \\
E_H(x) &= \frac{x(7x^2 - 29x + 16)}{36(x-1)^3} + \frac{x(3x-2)}{6(x-1)^4} \log x \\
E_\chi(x) &= \frac{(-11x^2 + 7x - 2)}{36(x-1)^3} + \frac{x^3}{6(x-1)^4} \log x
\end{aligned}$$

## References

- [1] A. Alavi-Harati et al., Phys. Rev. Lett. **83** (1999) 22.
- [2] V. Fanti et al., Phys. Lett. **B465** (1999) 335;  
A. Ceccucci, CERN Particle Physics Seminar (29 February 2000),  
<http://www.cern.ch/NA48/Welcome/images/talks/cern00/talk.ps.gz>.
- [3] H. Burkhardt et al., Phys. Lett. **B206** (1988) 169; G.D. Barr et al., Phys. Lett. **B317** (1993) 233.
- [4] L.K. Gibbons et al., Phys. Rev. Lett. **70** (1993) 1203.
- [5] S. Bosch, A.J. Buras, M. Gorbahn, S. Jäger, M. Jamin, M.E. Lautenbacher and L. Silvestrini, Nucl. Phys. **B 565** (2000) 3.
- [6] M. Ciuchini and G. Martinelli, hep-ph/0006056.
- [7] S. Narison, hep-ph/0004247.
- [8] J. Bijnens and J. Prades, JHEP **0006** (2000) 035.

- [9] M. Ciuchini, E. Franco, L. Giusti, V. Lubicz and G. Martinelli, hep-ph/9910237.
- [10] S. Bertolini, M. Fabbriehesi and J.O. Eeg, Rev. Mod. Phys **72** (2000) 65; hep-ph/0002234.
- [11] T. Hambye, G.O. Köhler, E.A. Paschos and P.H. Soldan, Nucl. Phys. **B 564** (2000) 391.
- [12] H.-Y. Cheng, hep-ph/9911202.
- [13] E. Pallante and A. Pich, Phys. Rev. Lett. **84** (2000) 2568; hep-ph/0007208.
- [14] A.A. Belkov, G. Bohm, A.V. Lanyov and A.A. Moshkin, hep-ph/9907335.
- [15] A.J. Buras, hep-ph/9908395; M. Jamin, hep-ph/9911390; U. Nierste, Nucl. Phys. Proc. Suppl. **86** (2000) 329.
- [16] E.A. Paschos, hep-ph/9912230.
- [17] A.J. Buras, M. Ciuchini, E. Franco, G. Isidori, G. Martinelli and L. Silvestrini, Phys. Lett. **B 480** (2000) 80.
- [18] L. Lellouch and M. Lüscher, hep-lat/0003023.
- [19] A.J. Buras, M. Jamin, M.E. Lautenbacher and P.H. Weisz, Nucl. Phys. **B 370** (1992) 69; Nucl. Phys. **B 400** (1993) 37. A.J. Buras, M. Jamin and M.E. Lautenbacher, Nucl. Phys. **B 400** (1993) 75. M. Ciuchini, E. Franco, G. Martinelli and L. Reina, Nucl. Phys. **B 415** (1994) 403.
- [20] A.J. Buras, M. Jamin and M.E. Lautenbacher, Nucl. Phys. **B 408** (1993) 209.
- [21] M. Ciuchini, E. Franco, G. Martinelli and L. Reina, Phys. Lett. **B 301** (1993) 263.
- [22] A.J. Buras, P. Gambino and U. Haisch, Nucl. Phys. **B 570** (2000) 117.
- [23] G. Buchalla, A.J. Buras and M. Lautenbacher, Rev. Mod. Phys **68** (1996) 1125.
- [24] A.J. Buras, hep-ph/9806471, hep-ph/9905437.
- [25] V. Cirigliano, J.F. Donoghue and E. Golowich, hep-ph/0007196.
- [26] S. Gardner and G. Valencia, Phys. Lett. **B 466** (1999) 355; hep-ph/0006240.
- [27] K. Maltman and C.E. Wolfe, hep-ph/0006091; hep-ph/0007061; Phys. Lett. **B 482** (2000) 77.



- [28] Y.-Y. Keum, U. Nierste and A.I. Sanda, Phys. Lett. **B457** (1999) 157.
- [29] A. Masiero and H. Murayama, Phys. Rev. Lett. **83** (1999) 907.
- [30] A.J. Buras, G. Colangelo, G. Isidori, A. Romanino and L. Silvestrini, Nucl. Phys. **B 566** (2000) 3.
- [31] A. Kagan and M. Neubert, Phys. Rev. Lett. **83** (1999) 4929.
- [32] G. Eyal, A. Masiero, Y. Nir and L. Silvestrini, JHEP 9911 (1999) 032.
- [33] X-G. He and B.H.J. McKellar, Phys. Rev. **D51** (1995) 6484; X-G. He, Phys. Lett. **B460** (1999) 405.
- [34] C-S. Huang, W-J. Huo and Y-L. Wu, hep-ph/0005227.
- [35] J. Agrawal and P. Frampton, Nucl. Phys. **B 419** (1994) 254.
- [36] F. Terranova, hep-ph/0005188.
- [37] E. Gabrielli and G.F. Giudice Nucl. Phys. **B433** (1995) 3; Erratum *Nucl. Phys.* **B507** (1997) 549.
- [38] E. Gabrielli, A. Masiero and L. Silvestrini, Phys. Lett. **B374** (1996) 80; F. Gabbiani, E. Gabrielli, A. Masiero and L. Silvestrini, Nucl. Phys. **B 477** (1996) 321.
- [39] G. Colangelo and G. Isidori, JHEP 09 (1998) 009.
- [40] A.J. Buras and L. Silvestrini, Nucl. Phys. **B 546** (1999) 299.
- [41] M.S Chanowitz, hep-ph/9905478(v2).
- [42] G. Buchalla, A.J. Buras and M.K. Harlander, Nucl. Phys. **B 349** (1991) 1; A.J. Buras and M.E. Lautenbacher, Phys. Lett. **B318** (1993) 212;
- [43] A.J. Buras, P. Gambino, M. Gorbahn, S. Jäger and L. Silvestrini, hep-ph/0007085.
- [44] S. Bertolini, F. Borzumati, A. Masiero and G. Ridolfi Nucl. Phys. **B353** (1991) 591.
- [45] M. Dugan, B. Grinstein and L. Hall, Nucl. Phys. **B255** (1985) 413.
- [46] L. J. Hall, V. A. Kostelecky and S. Raby, Nucl. Phys. **B267** (1986) 415.
- [47] F. Gabbiani and A. Masiero, Nucl. Phys. **B322** (1989) 235.

- [48] J. S. Hagelin, S. Kelley and T. Tanaka, Nucl. Phys. **B415** (1994) 293.
- [49] J. M. Frere, D. R. Jones and S. Raby, Nucl. Phys. **B222**, 11 (1983);  
 L. Alvarez-Gaume, J. Polchinski and M. B. Wise, Nucl. Phys. **B221**, 495 (1983);  
 J. P. Derendinger and C. A. Savoy, Nucl. Phys. **B237**, 307 (1984);  
 C. Kounnas, A. B. Lahanas, D. V. Nanopoulos and M. Quiros, Nucl. Phys. **B236**,  
 438 (1984).
- [50] M. Drees, M. Gluck and K. Grassie, Phys. Lett. **B157**, 164 (1985);  
 J. F. Gunion, H. E. Haber and M. Sher, Nucl. Phys. **B306**, 1 (1988);  
 H. Komatsu, Phys. Lett. **B215**, 323 (1988);  
 P. Langacker and N. Polonsky, Phys. Rev. **D50**, 2199 (1994).
- [51] J. A. Casas and S. Dimopoulos, Phys. Lett. **B387** (1996) 107 [hep-ph/9606237].
- [52] G. Buchalla, A.J. Buras, M.K. Harlander, M.E. Lautenbacher and C. Salazar, Nucl.  
 Phys. **B 355** (1991) 305.
- [53] G.C. Branco, G.C. Cho, Y.Kizukuri and N. Oshimo, Nucl. Phys. **B449** (1995) 483.
- [54] P. Cho, M. Misiak and D. Wyler, Phys. Rev. **D54** (1996) 3329.
- [55] A.J. Buras, M. Jamin, and P.H. Weisz, Nucl. Phys. **B347** (1990) 491.
- [56] S. Herrlich and U. Nierste, Nucl. Phys. **B419** (1994) 292, Phys. Rev. **D52** (1995)  
 6505, Nucl. Phys. **B476** (1996) 27.
- [57] J. Urban, F. Krauss, U. Jentschura and G. Soff, Nucl. Phys. **B 523** (1998) 40.
- [58] G. Ecker, G. Müller, H. Neufeld and A. Pich, Phys. Lett. **B 477** (2000) 88.
- [59] G. Buchalla and A.J. Buras, Nucl. Phys. **B548** (1999) 309; Nucl. Phys. **B 412**  
 (1994) 106.
- [60] A. J. Buras, M. E. Lautenbacher, M. Misiak and M. Münz, Nucl. Phys. **B423**  
 (1994) 349.
- [61] A.J. Buras, M.E. Lautenbacher and G. Ostermaier, Phys. Rev. **D50** (1994) 3433.
- [62] G. Buchalla and A.J. Buras, Phys. Lett. **B333** (1994) 221; Phys. Rev. **D54** (1996)  
 6872.
- [63] A.J. Buras, Phys. Lett. **B333** (1994) 476; Nucl. Instr. Meth. **A368** (1995) 1.

- [64] T. Goto, Y. Okada and Y. Shimizu, hep-ph/9908499.
- [65] A. Ali and D. London, Eur. Phys. J. **C9** (1999) 687.
- [66] CLEO coll., CLEO CON 98-17, ICHEP98-1011; Aleph coll., Phys. Lett. **B429** (1998) 169.
- [67] J. Erler and D. M. Pierce, Nucl. Phys. **B526** (1998) 53.
- [68] J. Ellis, T. Falk, G. Ganis and K. A. Olive, hep-ph/0004169.
- [69] R. Barbieri and G.F. Giudice Phys. Lett. **B 309** (1993) 86.
- [70] K. Chetyrkin, M. Misiak and M. Münz, Phys. Lett. **B400** (1997) 206; E: *ibid* **B425** (1998) 414; K. Adel and Y.P. Yao, Phys. Rev. **D49** (1994) 4945; C. Greub and T. Hurth, Phys. Rev. **D56** (1997) 2934; A.J. Buras, A. Kwiatkowski and N. Pott, Phys. Lett. **B414** (1997) 157 E: *ibid* **B434** (1998) 459; Nucl. Phys. **B517** (1998) 353;
- [71] M. Ciuchini, G. Degrossi, P. Gambino and G.F. Giudice, Nucl. Phys. **B 527** (1998) 21.
- [72] F. Borzumati and C. Greub, Phys. Rev. **D58** (1998) 074004; Phys. Rev. **D59** (1999) 057501.
- [73] A. Czarnecki and W.J. Marciano, Phys. Rev. Lett. **81** (1998) 277; A. Kagan and M. Neubert, Eur. Phys. J. **C7** (1999) 5; P. Gambino and U. Haisch, hep-ph/0007259.
- [74] M. Ciuchini, et al. Nucl. Phys. **B534** (1998) 3.
- [75] C. Bobeth, M. Misiak, J. Urban, Nucl. Phys. **B567** (2000) 153.
- [76] G. Cho and K. Hagiwara, Nucl. Phys. **B574** (2000) 623.
- [77] R. Barbieri and L. Maiani, Nucl. Phys. **B224** (1983) 32.
- [78] M. Drees and K. Hagiwara, Phys. Rev. **D42** (1990) 1709.
- [79] G. Altarelli, R. Barbieri and F. Caravaglios, Int. J. Mod. Phys. **A13** (1998) 1031; G. Altarelli, hep-ph/9811456.
- [80] J. Erler, hep-ph/9903449.
- [81] A. Djouadi, *et al.*, Phys. Rev. Lett. **78** (1997) 3626; Phys. Rev. **D57** (1998) 4179.

- [82] M. Carena *et al.*, Nucl. Phys. **B580** (2000) 29; J. R. Espinosa and R. Zhang, hep-ph/0003246.
- [83] LEP Higgs working group, see <http://lephiggs.web.cern.ch/LEPHIGGS/>.
- [84] S. Heinemeyer, W. Hollik and G. Weiglein, Phys. Lett. **B455** (1999) 179.
- [85] D. M. Pierce, J. A. Bagger, K. Matchev and R. Zhang, Nucl. Phys. **B491** (1997) 3; A. Dabelstein, Z. Phys. **C67** (1995) 495.
- [86] O. Schneider, hep-ex/0006006.
- [87] M. Carena, M. Quiros and C. E. Wagner, Phys. Lett. **B380** (1996) 81.